

# BIOGENESIS OF CHLOROPLAST MEMBRANES

## I. Plastid Dedifferentiation in a Dark-Grown Algal Mutant (*Chlamydomonas reinhardi*)

I. OHAD, P. SIEKEVITZ, and G. E. PALADE

From The Rockefeller University, New York 10021. Dr. Ohad's present address is the Department of Biological Chemistry, The Hebrew University, Jerusalem, Israel

### ABSTRACT

This paper describes the morphology and photosynthetic activity of a mutant of *Chlamydomonas reinhardi* (*y-1*) which is unable to synthesize chlorophyll in the dark. When grown heterotrophically in the light, the mutant is indistinguishable from the wild type *Chlamydomonas*. When grown in the dark, chlorophyll is diluted through cell division and the photosynthetic activity (oxygen evolution, Hill reaction, and photoreduction of NADP) decays at a rate equal to or faster than that of chlorophyll dilution. However, soluble enzymes associated with the photosynthetic process (alkaline FDPase, NADP-linked G-3-P dehydrogenase, RuDP carboxylase), as well as cytochrome *f* and ferredoxin, continue to be present in relatively high concentrations. The enzymes involved in the synthesis of the characteristic lipids of the chloroplast (including mono- and digalactoside glycerides, phosphatidyl glycerol, and sulfolipid) are still detectable in dark-grown cells. Such cells accumulate large amounts of starch granules in their plastids. On onset of illumination, dark-grown cells synthesize chlorophyll rapidly, utilizing their starch reserve in the process. At the morphological level, it was observed that during growth in the dark the chloroplast lamellar system is gradually disorganized and drastically decreased in extent, while other subchloroplast components are either unaffected (pyrenoid and its tubular system, matrix) or much less affected (eyespot, ribosomes). It is concluded that the dark-grown mutant possesses a partially differentiated plastid and the enzymic apparatus necessary for the synthesis of the chloroplast membranes (discs). The advantage provided by such a system for the study of the biogenesis of the chloroplast photosynthetic membranes is discussed.

### INTRODUCTION

Since membranes are currently recognized as "elementary structures" extensively used in the construction of a large number of cell organs, membrane biogenesis should be considered a basic process that underlies the differentiation, growth, and replication of many cell organs and of the cell itself. Some information is already available on the biogenesis—and its regulation—of whole cell organs, such as mitochondria and chloroplasts (1–

15), but these organs represent already complex structures in which membranes are only one of a series of components (16–19). Moreover, much of the recent literature (cf. (20, 21) for review) deals with local (satellite) DNA's and their possible function as autonomous or auxiliary genomes. Relevant to this paper is the discovery of satellite DNA's in *Chlamydomonas* (22–25). Information directly concerning operative and regulatory proc-

esses in membrane biogenesis is now needed in order to understand a basic step in biological organization: the transition from molecular to sub-cellular and cellular structures.

The study of membrane biogenesis would be facilitated by the availability of a system with the following characteristics: (1) synthesis of membranes at such rates as to allow adequate sampling time, and in quantities and configurations such as to permit isolation for biochemical analysis during the formative stages; (2) easy identification of the *new* cellular structures; (3) the membranes should have a distinct biochemical activity easily recognizable against the background of the metabolic activity of the cell and stable enough to permit assay *in vitro* after isolation; (4) the machinery necessary for the synthesis of membrane components should be present in a latent state and be activated by a simple physiological stimulus; (5) upon activation, the system should preferentially synthesize membrane components rather than increase all cellular synthetic activities.

These ideal requirements are met to variable degrees by etiolated plant leaves or algae in which the formation of chloroplast membranes is induced during the greening process. The greening process is defined here as the light-induced synthesis, in absence of cell division, of photosynthetic membrane components and their assembly into morphologically and biochemically distinct units.

The aim of this work is to characterize such a system using a dark-grown mutant of *Chlamydomonas reinhardi*, a unicellular alga with a single large plastid, as a generator of chloroplast membranes when exposed to light. In wild type *Chlamydomonas*, the cells have the ability to synthesize chlorophyll in the dark as well as in the light. It is, therefore, assumed that they, unlike Angiosperms among the higher plants and certain species of *Euglena* and *Ochromonas*, contain the entire enzymatic equipment necessary for this synthesis. The mutant in question apparently lacks part of this equipment, for if placed in the dark it will continue to grow and multiply, so that each cell will progressively lose its initial chlorophyll content. As will be shown below, this occurs by simple dilution through cell division of the chlorophyll originally synthesized in the light. Concomitantly, the discs of the chloroplasts disappear, though the chloroplast itself persists as a distinctive structure. Upon reexposure to light, these yellow cells will synthesize chlorophyll, by a light-activated step, and in-

crease the membrane content of their chloroplasts; all this happens without cell division. The structural and enzymic modulations that occur in the chloroplast of the mutant during "degreening," i.e. transition from the light-grown photosynthetic, to the dark-grown nonphotosynthetic state, form the subject of this paper. The analysis was carried out at the level of the whole cell with the intent to continue it at the chloroplast and chloroplast disc level in subsequent steps.

The results of experiments dealing with the reverse process ("greening"), i.e. the formation of the chloroplast disc system and reappearance of photosynthetic activity, will be reported in the accompanying paper.

## MATERIALS AND METHODS

### *Description of Mutant*

*Chlamydomonas reinhardi* wild type and *y-1* mutant were kindly supplied by Dr. R. Sager, Department of Biological Sciences, Hunter College, New York.

The mutant gene, *y-1*, arose as a spontaneous mutation. Although the mutation rate  $y-1^+$  to  $y-1^-$  is low, the reversion rate back to  $y-1^+$  is high, and stocks must be cloned regularly to maintain the purity of the mutant strain. *y-1* has been shown to behave as a single gene mutation, exhibiting 2:2 segregation in crosses, as expected for a unit factor (26). However, it is not yet established whether the location of the gene within the cell is chromosomal or nonchromosomal. Some genetic data suggest it to be nonchromosomal (27, 28), such as its response to streptomycin as a mutagen. Nonetheless, its pattern of unit-factor inheritance is different from the maternal inheritance found in the more than 40 different nonchromosomal genes so far identified in *Chlamydomonas* (29). There are only few data as to the biochemical lesion involved in the single-gene mutation of *y-1*; that available suggest a block between protochlorophyll(ide) and chlorophyll(ide) (30), but a block at an earlier point is not excluded.

Mutant cells grown in the dark or light will be referred to hereafter as chyd cells and chyl cells, respectively.

### *Culture of Algae*

The cells were grown in a medium which is similar to that described by Sager and Granick (31) and has the following composition: 1000-ml solution A (Na citrate,  $1.7 \times 10^{-3}$  M; Na acetate,  $7.5 \times 10^{-3}$  M;  $K_2HPO_4$ ,  $5.7 \times 10^{-4}$  M;  $KH_2PO_4$ ,  $7.4 \times 10^{-4}$  M;  $NH_4NO_3$ ,  $3.7 \times 10^{-3}$  M;  $MgSO_4$ ,  $1.2 \times 10^{-3}$  M;  $CaCl_2$ ,  $3.6 \times 10^{-4}$  M;  $FeCl_3$ ,  $3.7 \times 10^{-5}$  M) supplemented with 1-ml solution B (a trace-metal solution consisting of (mg/100 ml):  $H_3BO_3$ , 100;  $ZnSO_4 \cdot 7$

H<sub>2</sub>O, 100; MnSO<sub>4</sub>·H<sub>2</sub>O, 40; CoCl<sub>2</sub>·6 H<sub>2</sub>O, 20; Na<sub>2</sub>MoO<sub>4</sub>·2 H<sub>2</sub>O, 20; CuSO<sub>4</sub>·5 H<sub>2</sub>O, 6.25). A five-times concentrated stock solution of medium A could be kept at 4° for 1–2 wk, the trace metals B being added only before autoclaving, which was carried out at 15 psi for 20 min for volumes up to 2 l, and for 40 min for volumes of 2–15 l.

Stock cultures were kept on agar slants prepared by adding 2% agar (Difco) to the above medium. These stock cultures were maintained by transferring to fresh agar medium every 4–6 days.

All liquid culture incubations were at 25° either in the dark or light (~700 ftc) in a photosynthetic incubator (New Brunswick incubator shaker, model G-27) operated at one shaking cycle/second and provided with white fluorescent lamps.

Mass liquid cultures of chyd cells were initiated by inoculating a loop of cells from a 2- to 4-day old agar-slant culture into an Erlenmeyer flask containing 100 ml of liquid medium and allowing growth in the light for two to three generations (usually overnight). Fernbach flasks containing 2 l of medium were inoculated with these 100 ml of liquid cultures to give an initial cell count of ~10<sup>4</sup> cells/ml. A mixture of 5% CO<sub>2</sub> in air (Matheson Co., East Rutherford, N. J.) was bubbled through the culture after passing through a sterilized cotton filter, and the flasks were incubated in the dark for 5–7 days.

For mass culture in liquid medium in the light (chyl cells), a sterile semicontinuous culture apparatus was used consisting of a reservoir (15 l) and a culture flask equipped with a ground-glass inlet to allow replenishing with fresh medium and a ground-glass outlet at the bottom to drain periodically the contents of the vessel (Fig. 1). The initial inoculation was with two to three loops of cells grown in the light on agar slants. For logarithmic growth, the culture was harvested every 24 hr by leaving in the growing flask only 100–200 ml of the old culture and replenishing the volume with 2 l of fresh medium. By this method, it was possible to have a continuous supply of cells (2–8 × 10<sup>9</sup> cells/day) for as long as 2–3 wk, at which time bacterial contamination eventually occurred and the process had to be started again.

### *The Degreening Process*

This was followed by growing the cells in the semicontinuous culture apparatus described above. The cells were first grown in continuous light (about 700 ftc) up to a concentration of ~1.3 × 10<sup>6</sup> cells/ml, then half the volume was drained (1.25 l) and used for enzyme assays and morphological studies. The volume of the culture was brought up to 2.5 l with fresh medium (final cell concentration ~0.8 × 10<sup>6</sup> cells/ml), and the incubation continued in the dark for the rest of the experiment. Every 22–24 hr, an adequate volume of the culture was withdrawn, as

described above, so as to bring the cell concentration, after replenishing with fresh medium, to the original value of ~0.8 × 10<sup>6</sup> cells/ml. Under these conditions, the generation time in the dark was approximately 22 hr as compared with 18–20 hr in the logarithmic phase of growth. Three culture flasks were used for each experiment. Since variation in chlorophyll content and cell count did not exceed 10% from one flask to another, the cells harvested from all three flasks were pooled for enzymic and morphological analysis.

### *The Greening Process*

This was followed by incubating chyd cells in the culture medium at final concentration ranging from 1 × 10<sup>6</sup> to 2 × 10<sup>7</sup> cells/ml. The ratio, surface-to-volume, in the incubation vessel was about 0.5–0.7 cm<sup>-1</sup>. Illumination was provided by white fluorescent lamps supplying about 700 ftc at the level of the cell suspension.

Bacterial contamination was checked by examining at various time intervals in the phase-contrast microscope pellets obtained by centrifuging the cultures at 10,000 *g* for 5 min. No significant contamination occurred during the 6–12 hr of the greening process.

Cells were harvested by centrifugation at 3000 *g* for 2 min in the cold, washed with fresh medium (~20 ml of medium per 1 ml of packed cells), recentrifuged, and then kept in ice until used (10–20 min). The number of cells in the sample was estimated by counting in a hemocytometer.

During the preparation steps, chyd cells were occasionally exposed to dim artificial or natural light for periods of <math>\lesssim 15</math> min in the cold. Special care to avoid such exposure was unnecessary, since chilled cells kept in the light for up to 1 hr showed neither increase in the amount of chlorophyll, nor changes in their morphology as compared with nonexposed cells.

### *Preparation of Homogenates*

Homogenates for enzymic assays were prepared by first washing the cells in the appropriate enzyme assay buffers (~20 ml of buffer solution per 1 ml of packed cells) and then disrupting them at a final concentration of 2 × 10<sup>8</sup> cells/ml in a French press (32) fitted with an oil pump and accessory valve (Blackhawk Industrial Products Co., Butler, Wis.) designed to insure a constant pressure (5000 psi) throughout the process. Under these conditions, all the cells and practically all the chloroplasts were completely fragmented, as ascertained by light and electron microscopy.

### *Enzyme Assays*

All the activities or concentrations are expressed on a per cell basis, rather than on a protein basis, since the protein concentrations vary during the greening

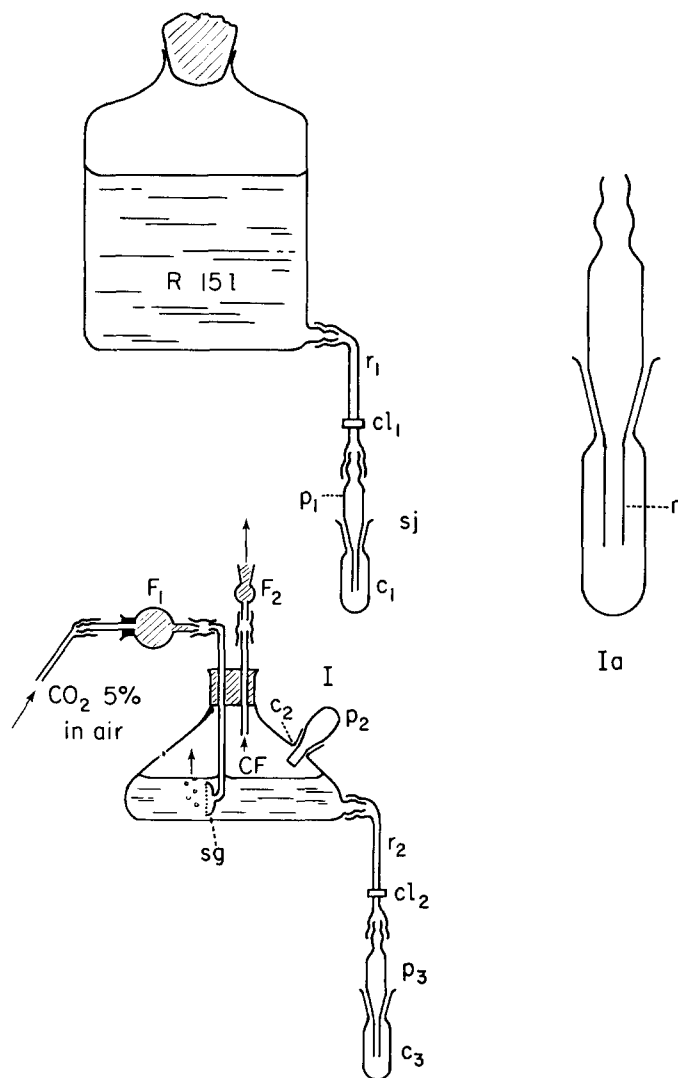


FIGURE 1 Apparatus for semicontinuous culture of algal cells. The reservoir (*R*) was connected through the ground-glass sterile joints (*sj*) with the inlet (*I*) on the culture flask (*CF*). This was done by removing cover *c*<sub>1</sub> from plug *p*<sub>1</sub>, inserting plug *p*<sub>1</sub> into inlet *c*<sub>2</sub> and then opening the clamp (*cl*<sub>1</sub>). Bubbling of CO<sub>2</sub>-air mixture, sterilized by passage through the cotton filter *F*<sub>1</sub> and dispersed by the sintered glass filter (*sg*), provided positive pressure in the culture flask preventing contamination when inlet (*I*) was open. Air escapes through filter *F*<sub>2</sub>. Drainage of culture was carried out through outlet *c*<sub>3</sub> and clamp *cl*<sub>2</sub>. An enlarged view of the ground-glass connection tube is shown in Fig. 1 *a*. The long neck (*n*) of plugs *p*<sub>1</sub> and *p*<sub>3</sub> allow passage of liquid without wetting the ground joints, thus ensuring sterility. The rubber connections (*r*<sub>1</sub> and *r*<sub>2</sub>) were of latex surgical tubing which can withstand autoclaving three to five times. All the ground-glass joints were of pyrex glass. The joints were sterilized by glowing over a Bunsen flame each time the covers were removed.

process, but cell number remains invariant. Respiration and oxygen evolution were measured in a Warburg apparatus with the use of incandescent lamps providing ~500 ftc at the level of the vessels.

The cells were resuspended in the growing medium at a concentration of 10<sup>8</sup> cells/ml, and O<sub>2</sub> uptake was followed in the dark and light in the presence of 10 N KOH in the center well. For oxygen evolution

measurements, the cells were resuspended in a 1:1 mixture of 0.07 M  $\text{KHCO}_3$  and 0.11 M  $\text{NaHCO}_3$ , pH 8.4, and saturated with  $\text{CO}_2$  by bubbling a mixture of 5%  $\text{CO}_2$  in air (33). The specific rate of oxygen evolution ( $\mu\text{mole}/\text{min}/10^8$  cells) was dependent on cell concentration in the range of  $2 \times 10^8$  to  $2 \times 10^7$  cells per ml (or  $6 \times 10^7$  cells per flask). This was probably because of insufficient illumination at high cell concentrations. Measurements were, therefore, performed at those concentrations at which the response was proportional to cell concentration, and extrapolated to  $10^8$  cells per flask.

Succinic dehydrogenase was measured in homogenates, as described by Bernath and Singer (34).

The alkaline FDPase<sup>1</sup> was assayed as described by Racker and Schroeder (35) and Smillie (36) in a system containing in 1.0 ml final volume: 10  $\mu\text{moles}$  fructose 1-6 diphosphate; 10  $\mu\text{moles}$   $\text{MgCl}_2$ ; 3  $\mu\text{moles}$  EDTA; 100  $\mu\text{moles}$  Tris buffer, pH 8.8; and the requisite amount of homogenate. The reaction was carried out at room temperature (26–28°) for 30 min and stopped by adding TCA to a final concentration of 10%. Inorganic phosphate in the acid-soluble supernatant was determined by the Fiske-SubbaRow method (37).

The NADP-linked G-3-P dehydrogenase was assayed as described by Smillie and Fuller (38) in 3.0 ml final volume containing: 100  $\mu\text{moles}$  of Tris buffer, pH 8.0; 50  $\mu\text{moles}$  of Na arsenate; 60  $\mu\text{moles}$  of NaF; 15  $\mu\text{moles}$  of cysteine, pH 8.0; 0.2  $\mu\text{mole}$  of NADP; 10  $\mu\text{moles}$  of G-3-P; and the requisite amount of homogenate. The reaction was run at room temperature in a Beckman DU spectrophotometer with a Gilford recording attachment by first preincubating all ingredients except substrate for 10 min, and then adding the substrate. Optical density changes were read at 340  $m\mu$ ; the rate was calculated from the linear part of the curve, with  $6.22 \times 10^6/\text{cm}^2/\text{mole}$  as the extinction coefficient for NADPH.

The photoreduction of NADP (39) was carried out by incubating at room temperature, in a Beckman DU spectrophotometer cuvette: 30  $\mu\text{moles}$  of Tris buffer, pH 7.5, 1  $\mu\text{mole}$  of  $\text{MgCl}_2$ , 0.2  $\mu\text{mole}$  of NADP, a spinach extract (~1 mg protein) containing ferredoxin, and the requisite amount of homogenate in a final volume of 3.0 ml. The light source was an incandescent lamp ( $\approx 700$  ftc) placed before a 10-cm

<sup>1</sup>The following abbreviations were used in this paper: FDPase, fructose-1,6-diphosphatase; RuDP, ribulose-1,5-diphosphate; RuDP carboxylase, ribulose-1,5-diphosphate carboxylase; DCI, dichlorophenol indophenol; ftc, foot candle; ER, endoplasmic reticulum; PPN reductase, photosynthetic pyridine nucleotide reductase; EDTA, ethylenediaminetetraacetate; G-3-P, glyceraldehyde-3-phosphate; TCA, trichloroacetic acid; NADP, nicotinamide adenine dinucleotide phosphate.

deep water bath; illumination was for 30-sec intervals, with readings in the dark at 340  $m\mu$ ; a dark-blank of similar composition but covered with aluminum foil was always run, and the readings subtracted from those of the light-activated samples. There was no reaction in the light without the added ferredoxin. The source of the ferredoxin was the dialyzed extract of the acetone precipitate prepared from spinach as described by San Pietro and Lang (39). In measuring the appearance of NADP photoreduction during greening, the above assay conditions were used with equal amounts of spinach ferredoxin extract added at all time points. In the assay for ferredoxin activity in *Chlamydomonas*, a similar extraction (39) was performed on packed green or yellow cells and the extract assayed as described above, with a dilute homogenate of green cells as a source of the light-activated reaction. In this manner, a quantitative measure of ferredoxin activity was made by measuring the rate of NADP photoreduction catalyzed by an extract from  $10^9$  chyl or chyd cells. Rates in both assays were calculated from the linear parts of the curves, and all activities were expressed as  $\mu\text{moles}$  NADP reduced.

RuDP carboxylase was measured as described by Smillie (40) in a reaction mixture of 0.5 ml final volume containing 12  $\mu\text{moles}$  of Tris buffer, pH 8.0, 5  $\mu\text{moles}$  of  $\text{MgCl}_2$ , 0.15  $\mu\text{mole}$  of EDTA, 3  $\mu\text{moles}$  of glutathione, 1  $\mu\text{mole}$  of RuDP (Sigma Co.), 1, 3, or 5  $\mu\text{moles}$  of  $\text{Na}^{14}\text{CO}_2$ , and the requisite amount of homogenate. The larger amounts of radioactive  $\text{CO}_2$  were used in the comparison of light-grown and dark-grown cells, in order to overcome somewhat the radioactivity dilution effect by different amounts of nonradioactive  $\text{CO}_2$  in the two cases. Reactions were run at room temperature for 5 and 10 min, with varying amounts of homogenate and with a blank lacking substrate. At the end of the incubation, 1.5 ml of boiling 70% alcohol were added, along with two drops of glacial acetic acid; the reaction vessels were heated for 1 min in a boiling water bath, cooled, and aliquots were plated for counting. Linear rates were obtained with time and tissue concentration after correcting for zero time control and a blank without substrate.

The Hill reaction was measured according to James and Das (41) in a system containing 30  $\mu\text{moles}$  of phosphate buffer, pH 6.6, 17  $\mu\text{moles}$  of KCl, 0.1  $\mu\text{mole}$  of DCI, and different amounts of homogenate in a final volume of 3.0 ml. Light was shown as above in 30-sec intervals and the change in OD at 600  $m\mu$  measured with a Zeiss spectrophotometer; a dark control and a control with *o*-phenanthroline (0.4  $\mu\text{mole}$ ) were always run. The rates were linear with time and homogenate concentration after subtracting the values of the dark control.

### Chemical Determinations

Total chlorophyll was measured in 80% acetone extracts of the harvested cells or homogenates as described by Arnon (42).

Cytochrome *f* was measured by the method of Chance (43) as described by Hill and Bonner (44, 45), using a split beam or double beam spectrophotometer, and recording in liquid nitrogen or at room temperature the difference spectra (ox/red) of 80% acetone-extracted cells suspended in 0.1 M Naphosphate buffer, pH 7.4.<sup>2</sup>

Total lipids were extracted from the whole cells and chromatographed after deacylation as described by Wintermans (46). The resolved deacylated mono- and digalactosylglycerides were identified with the aid of purified radioactive markers (kindly donated by Dr. A. A. Benson, Scripps Institute, La Jolla, Calif.) on radioautograms of the chromatograms, and by staining with the Schiff reagent.<sup>3</sup> Two-dimensional

<sup>2</sup> We are very thankful to Dr. Walter D. Bonner, Johnson Foundation, University of Pennsylvania, for performing these determinations, and interpreting the results.

<sup>3</sup> A modification of Schiff reaction was kindly supplied by Dr. M. Kates, National Research Council, Ottawa, Canada.

chromatography of nondeacylated lipids was carried out on commercial silicic acid-impregnated paper (Whatman, No. SG 81) with the use of the solvent systems described by Marinetti (47). The nondeacylated phospholipids and sulfolipids were located by using extracts of cells preincubated in the light either with  $^{32}\text{PO}_4^{3-}$  or  $^{35}\text{SO}_4^{2-}$  and comparing the radioautograms with those of lipids extracted from  $^{14}\text{C}$ -labeled cells. There was only one spot on the  $^{35}\text{S}$ -labeled radioautogram, presumably the sulfolipid described by Benson et al. (48). The individual phospholipids were tentatively identified by their location (46, 47). Monogalactosylglyceride distearate (kindly supplied by Dr. M. Kates, National Research Council, Ottawa, Canada) served as a marker for the monogalactosyl lipid. There were only two spots staining with the Schiff reagent, one identified with the monogalactosyl marker, and the other corresponding to the position of the digalactosyl lipid (46). The pattern of the chromatograms was highly reproducible and corresponded well with that of plant lipids shown by Marinetti (47).

Incorporations of  $^{32}\text{PO}_4^{3-}$ ,  $^{35}\text{SO}_4^{2-}$ , or  $^{14}\text{C}$ -acetate by the algae in the dark or light were carried out by the same procedure as for the greening experiments. The radioactive material (amount noted in figure legends) was added to the incubation medium at the zero time of the experiments. Analyses for protein and

---

All micrographs show sections of *Chlamydomonas reinhardtii* cells fixed in 2%  $\text{OsO}_4$  in 0.1 M phosphate buffer (pH 7.2), embedded in Epon, and sectioned at  $\approx 500$  Å with diamond knives. The sections were doubly stained with  $\text{UO}_2$  acetate and Pb citrate and micrographed in a Siemens Elmiskop I.

### General Abbreviations

*ce*, chloroplast envelope; *cm*, chloroplast matrix; *cr*, chloroplast ribosomes; *d*, disc; *db*, bent or folded over disc; *dc*, dictyosome; *m*, mitochondrion; *mb*, cell membrane; *n*, nucleus; *ne*, nuclear envelope; *no*, nucleolus; *o*, osmiophilic globule; *p*, pyrenoid; *r*, cytoplasmic ribosomes; *rer*, rough-surfaced endoplasmic reticulum; *sg*, starch granules; *sp*, starch plates; *t*, pyrenoid tubules; *v*, vacuole; *w*, cell wall.

FIGURE 2 General morphology of a mutant cell grown in the light (chyl) in batch type culture. The figure shows the profile of a medially sectioned cell whose cell wall is marked *w* and cell membrane *mb*. The cup shape of the chloroplast and the location of the pyrenoid (*p*) within the thickened posterior part of the plastid are clearly shown. The chloroplast is bounded by chloroplast envelope (*ce*) (see Fig. 5 for further detail) and contains many grana (*g*), i.e., stacks of fused discs connected by one or more free or fused discs. Osmiophilic globules (*o*) and a few starch granules (*sg*) are scattered among the grana.

The pyrenoid (*p*) appears as a large, finely granular mass of polygonal profile surrounded by discontinuous shell of starch plates (*sp*) and penetrated by a system of tubules (*t*). Within the chloroplast cup are located the nucleus (*n*), dictyosomes (*dc*) and their associated vacuoles (*v*), and endoplasmic reticulum cisternae of transitional type (*tc*). Mitochondria (*m*) are concentrated at the anterior pole of the cell and between the chloroplast and the cell membrane. A contractile vacuole is marked *cv* and a flagellum *fl*.  $\times 20,000$ .



lipid were carried out as described in the following paper (49).

Insoluble starch was measured in the residue after acetone extraction of whole cells. The residue was washed twice with 2%  $\text{Na}_2\text{CO}_3$ , and recovered each time by centrifuging at 3000 *g*, 5 min. Since the cell wall was not disrupted by this procedure, all starch granules were retained inside the sac formed by the cell wall, thereby allowing good recovery at low-speed centrifugation. The sediment was hydrolyzed in  $\text{N H}_2\text{SO}_4$  at 100° for 10 min and the amount of total sugar was determined in the 3000-*g*, 5-min supernate of the hydrolysate by using the phenol-sulfuric acid reagent of Dubois et al. (50). The same values were obtained if hydrolysis was carried out at pH 2, for 20 min. Since the cellulosic cell wall is not significantly affected by  $\text{N H}_2\text{SO}_4$  even after more prolonged exposure,  $\text{H}_2\text{SO}_4$  was consistently used to ensure complete dissolution of the starch. Starch granules were isolated for identification from homogenates prepared in 0.04 M Tris buffer, pH 7.4, at 5000 psi. The homogenate, centrifuged at 15,000 *g* for 20 min, yielded a hard white pellet overlaid by a fluffy pigment-rich layer. The latter was easily removed by gentle pipetting with 2%  $\text{Na}_2\text{CO}_3$ . The white pellet was then resuspended in 2%  $\text{Na}_2\text{CO}_3$ , washed twice as above, and finally extracted with 80% acetone. The residue was a white powder consisting of strongly refractile granules of varying size (0.3–2  $\mu$ ). It was identified as starch by acid hydrolysis at pH 2 (10 min, 100°) which yielded glucose and traces of maltose and higher oligosaccharides, or by  $\alpha$ -amylase (hog pancreas, Worthington) hydrolysis which gave maltose and small amounts of glucose. The identification of the hydrolysis products was made by descending paper chromatography in *N*-propanol-ethylacetate-water (7/3/1 by volume) with a benzidine reagent for detection (51).

### Preparation of Specimens for Electron Microscopy

Whole cells were fixed in 2%  $\text{OsO}_4$  in 0.1 M phosphate buffer, pH 7.4, or in 2% glutaraldehyde in 0.2 M cacodylate buffer, pH 7.4, containing  $2 \times 10^{-3}$  M  $\text{CaCl}_2$  or  $\text{MgCl}_2$ . Fixation was at 4° for overnight. Specimens fixed in the last fixative were washed and postfixed overnight in 2%  $\text{OsO}_4$  in the same buffer. Some of the specimens were stained in block with 0.5% uranyl acetate in acetate Veronal buffer, pH 6.0, before dehydration.

After fixation, specimens were dehydrated in a series of graded alcohols and finally embedded in Epon as in Luft's procedure (52). Sections were cut with a Porter-Blum Servall MT2 microtome using a diamond knife (DuPont de Nemours, Wilmington, Del.), and were mounted on 200-mesh grids coated with a formvar film or on naked 400-mesh grids. The sections were stained with uranyl acetate and lead citrate, as described by Reynolds (53), and then covered with a thin film of carbon. A Siemens Elmiskop I was used at magnifications of 6,000 to 60,000.

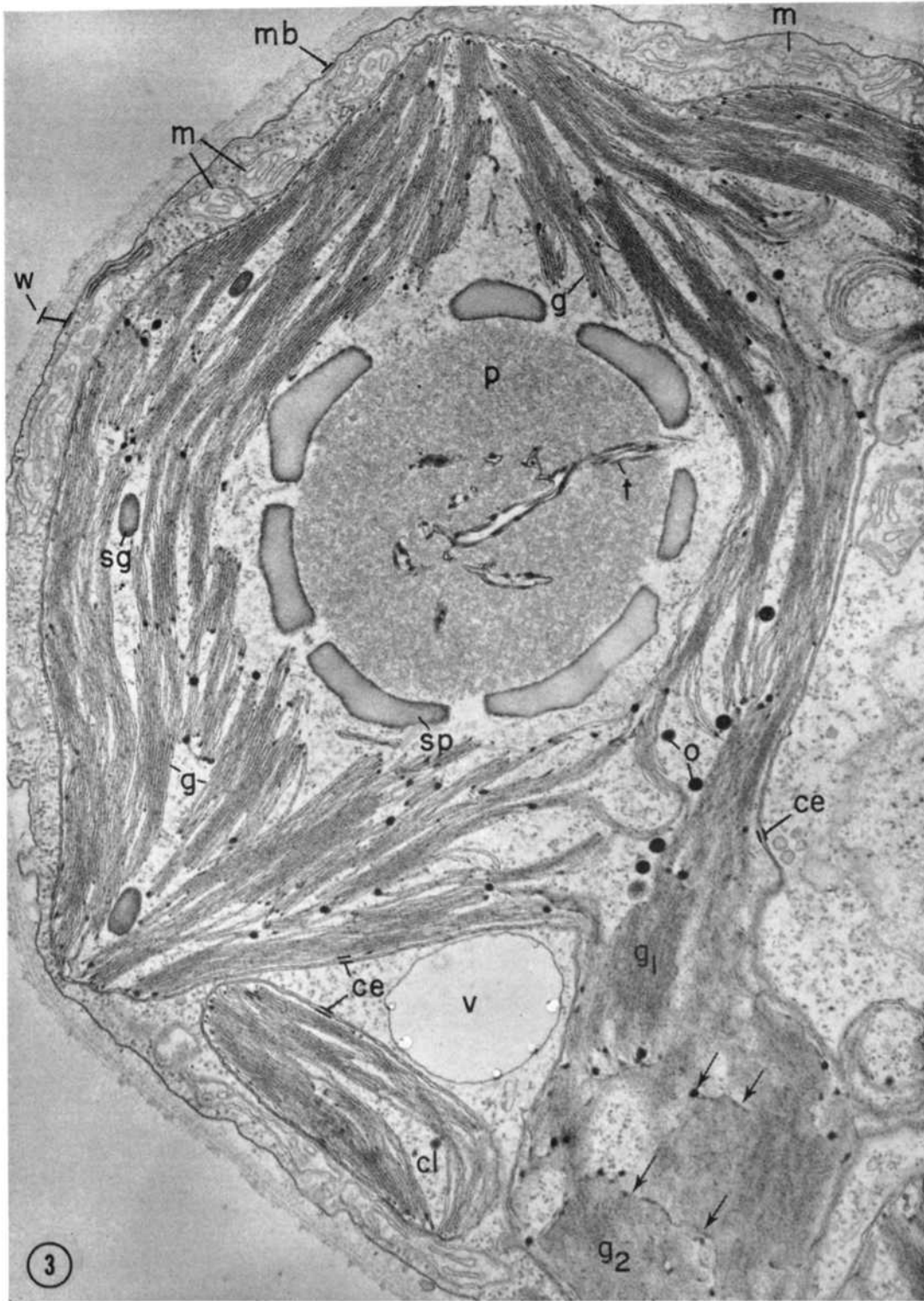
The amount of membranes forming the lamellar system of the chloroplast, and the incidence of fusion lines of grana were estimated from electron micrographs with the use of a procedure similar to that described by Loud (54). Randomly taken electron micrographs (magnifications, 30,000 to 40,000) of sections including comparable amounts of the chloroplast area were scanned with a grid having a spacing of 1  $\mu$ . The scanning was done on prints enlarged to  $\times 100,000$ . The membrane content index is defined as the number of intersections of membrane profiles or grana fusion lines with the grid lines divided by the surface of the chloroplast area scanned.

---

FIGURE 3 Mutant cell grown in the light in batch type culture. Section cutting through the center of the bottom of the chloroplast cup. The chloroplast is bounded by a chloroplast envelope (*ce*) and is occupied by numerous grana, each formed by a pile of fused discs. Most grana are perpendicularly sectioned (*g*); a few appear in oblique (*g*<sub>1</sub>) and grazing (*g*<sub>2</sub>) sections. The latter show a full-faced view of the large festooned discs and show clearly the irregularly thickened disc rims (arrows). Such thickened rims appear as dense dots at the end of many normally sectioned discs throughout the chloroplast. In addition to those fused into grana, a few free or intergranar discs are present. The space among the grana is occupied by a relatively tight matrix (stroma) which contains osmiophilic globules (*o*), starch granules (*sg*), and numerous ribosomes. (The latter are hardly visible at this magnification; see, however, Figs. 10 and 11.)

The pyrenoid (*p*) occupies the center of the chloroplast bottom and consists of a finely granular core surrounded by a discontinuous shell of starch plates (*sp*) and penetrated by a network of tubules (*t*). The profile marked *cl* is part of the irregularly deeply cut rim of the chloroplast cup.  $\times 27,000$ .





An average of 1700 cm<sup>2</sup> was scanned at each time point.

## RESULTS

### *Growth Characteristics of Light-Grown and Dark-Grown Cells*

The generation time of both wild type and mutant cells was found to be 18–20 hr when grown in the dark and  $\approx 6$  hr when grown in continuous light. Logarithmic growth was maintained in all cultures up to concentrations of  $\sim 2 \times 10^6$  cells/ml. The concentration of chlorophyll in chyl cells in logarithmic growth was 18–20  $\mu\text{g}/10^7$  cells, increasing in the stationary phase to 30–50  $\mu\text{g}/10^7$  cells. The chlorophyll content of chyd cells was  $\leq 0.3 \mu\text{g}/10^7$  cells after seven to nine generations of growth in the dark.

When attempts were made to grow chyd cells in liquid semicontinuous culture, it was found that often the culture deteriorated and cell death became apparent after 14 to 18 generations. The cells of the original culture were sometimes slowly replaced by what seems to be a back mutant which is able to synthesize chlorophyll in the dark, thus being similar to the wild type. Green colonies were observed also in cultures grown in the dark on agar plates whenever these cultures were not transferred to new medium within 2–3 wk. The back mutant, however, does not accumulate in light-grown liquid cultures during as many as 50 to 60 generations, as tested by inoculating cells from such cultures on agar slants or liquid cultures and allowing growth in the dark.

### *Morphology of the Mutant Grown in Light and Dark*

Mutant cell populations during the logarithmic phase of growth in either light or dark were homogeneous as observed in the light and electron microscopes. When grown in the light, the cells were ellipsoidal with a short axis of 5–8  $\mu$  and a long axis of 8–12  $\mu$ ; cells grown in the dark were more rounded. Both chyl and chyd cells were motile and did not form clumps or aggregates.

At the electron microscopic level, the morphology of chyl cells was, in general, similar to that of chyd cells except for the lamellar system of the chloroplast and its starch content. In the following description, the structure of both light- and dark-grown cells would be considered together except for the intrachloroplast membranes.

The cell is contained within a cell wall of varying thickness (0.1–0.2  $\mu$ ) and fibrillar texture (Figs. 2 and 3) which in normal sections can be resolved into as many as six to ten layers of fibrils. In each layer, the fibrils are oriented parallel to one another, but from one layer to the next their orientation changes by a large angle. The thickness of the fibrils is  $\sim 30$  A, as expected for single cellulose elementary fibrils (55). The space between adjacent fibril layers appears to be “empty” (i.e., occupied only by embedding plastic). Whether this free space is present also *in vivo*, or is the result of extraction of soluble components during specimen preparation, is not known.

The cell membrane consists of a single unit membrane  $\approx 100$  A in thickness. Its outer dense leaflet is usually thicker and more intensely stained than the inner dense leaflet (Figs. 3 and 7). The cell

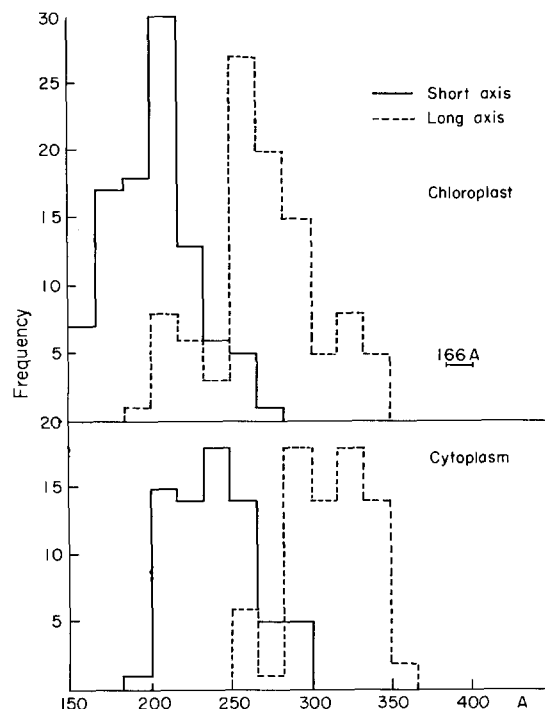


FIGURE 4 Size distribution of cytoplasmic ribosomes and of ribosome-like particles in chloroplasts of light-grown mutants. The particles are slightly elongated. Full line, short axis; dotted line, long axis. *A*, chloroplast particles; *B*, cytoplasmic ribosomes. Measurements were made with a magnifier ( $\times 10$ ) on micrographs taken at 40,000 electron magnification, enlarged photographically to 100,000. The same cell sections were used for measurement of both kinds of particles. The data were collected from a total of ten micrographs.

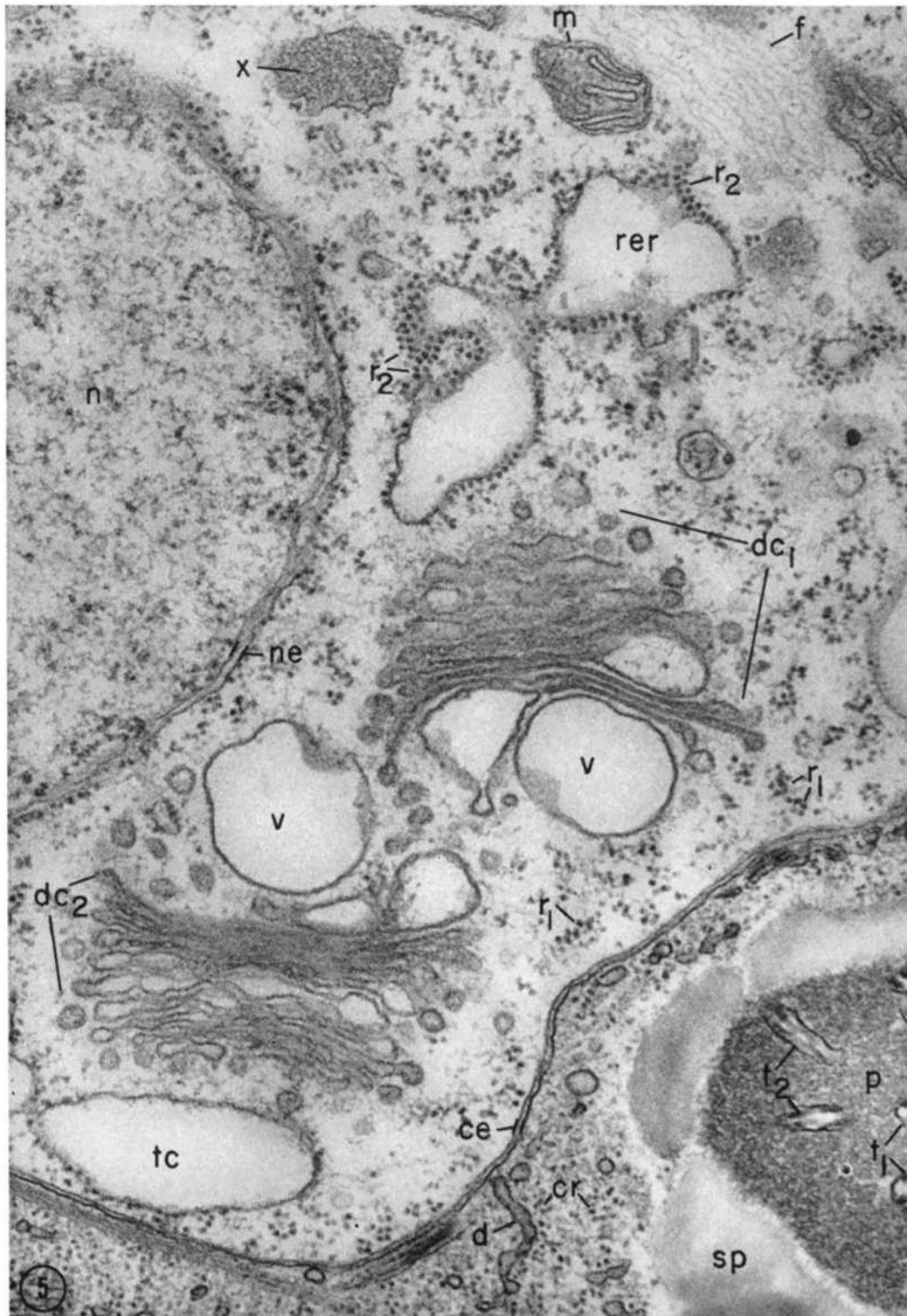


FIGURE 5 Small field in a dark-grown cell in the vicinity of the nucleus. Two dictyosomes ( $dc_1$ ,  $dc_2$ ) with their piled cisternae, small smooth-surfaced vesicles, and central vacuoles ( $v$ ) are located behind the nucleus at the bottom of the chloroplast cup. The associated transitional cisterna of  $dc_2$  is seen at  $tc$ ; while a dilated cisterna of the rough endoplasmic reticulum ( $rer$ ), whose attached ribosomes are disposed in patterns, primarily double rows ( $r_2$ ), appears near  $dc_1$ . A bundle of fine filaments and a membrane-bounded granule with a dense homogeneous content are seen at  $f$  and  $x$ , respectively. Such granules occur in all cells (see Figs. 2 and 12) but their nature and function is unknown.  $\times 57,000$ .

membrane is found either in direct apposition to the cell wall or retracted and folded forming invaginations 0.2–0.5  $\mu$  deep which may reflect a normal condition of the cell or a certain degree of plasmolysis. In poorly preserved material, the invaginations are much more extensive, the membrane is often ruptured, and myelin figures develop in the space between the cell wall and the cell membrane.

The cytoplasm consists of a relatively light matrix in which are scattered many ribosomes that appear as slightly elongated bodies having a short axis of  $232 \pm 33$  A and a long axis of  $315 \pm 25$  A (Fig. 4). The ribosomes exist either individually or in clusters; most are free, only a few being attached to the external surface of the nuclear envelope as well as to membranes which limit the few cisternal elements of the endoplasmic reticulum of this cell. In both locations, the attached ribosomes are disposed in patterns, e.g., double rows, circles, and rosettes (Fig. 5).

The nucleus, round-to-ovoid in shape, has a diameter of 2–3  $\mu$ , and is located deep within the plastid cup. The nuclear envelope consists, as usual, of two unit membranes separated by a light space of variable width (80–200 A) and traversed by nuclear pores  $\sim 800$  A in diameter. A single, spherical (diam.  $\simeq 1.2$   $\mu$ ), central nucleolus is present which consists of a shell of dense granules ( $\sim 200$  A) and a core of dense, finely fibrillar material (Fig. 12). Masses of packed dense fibrils occur in the nucleus, either immediately under the nuclear envelope or scattered in the nucleo-

plasm. The latter has a loose fibrillar texture and contains a relatively large population of granules of varied size and density (Fig. 12).

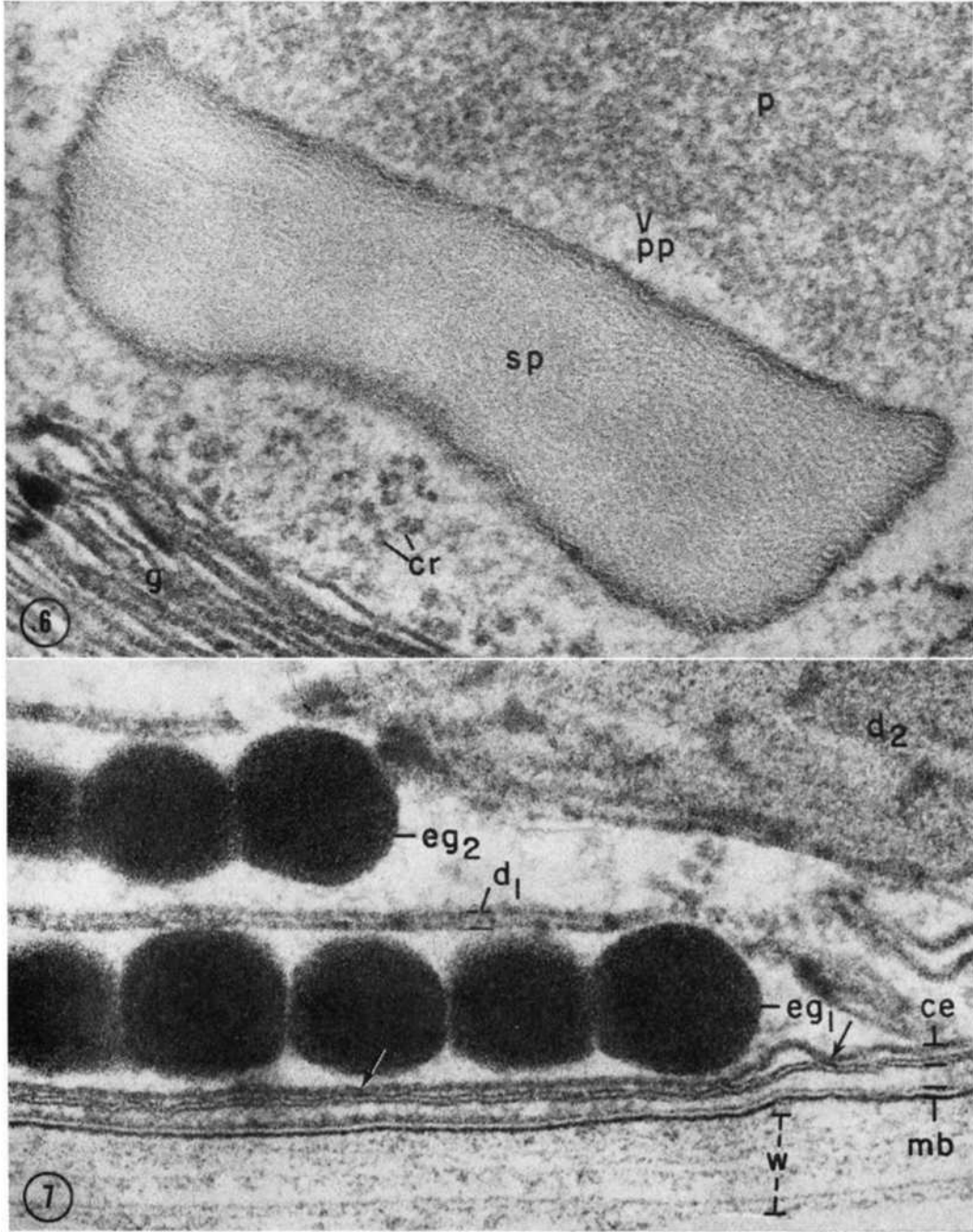
Between the nucleus and the chloroplast cup is located a single row of dictyosomes, each consisting of eight to fifteen piled cisternae (Fig. 5). In profile, the margin of the cisternae is distended or vesiculated; in full faced view they are circular, measuring 1–1.5  $\mu$ , and show vesiculated borders. Each dictyosome is polarized in the sense that the side of the pile facing the nucleus is made up of one to three cisternae with asymmetric membranes. The asymmetry is reminiscent of that of the cell membrane and is shared by a number of vacuoles and multivesicular bodies located in the immediate vicinity of the stack. The other end of the pile has cisternae with symmetrical membranes and usually abuts against a transitional element, part rough and part smooth, of the ER. Small, smooth-surfaced vesicles, of the type seen in other cells at the periphery of the Golgi complex, are seen at this level. They are frequently in contact or continuity with the transitional element, which often appears distended. The images suggest that the small vesicles fuse with, or form by budding from, the transitional cisterna.

In general, five to ten mitochondrial profiles of usual appearance and round-to-elongate shape are found per cell section. Most of them are located in the apical region of the cell, and peripherally between the chloroplast and the cell membrane (Figs. 2 and 3). The mitochondria are larger and have more cristae in dark-grown cells (Fig. 12).

---

FIGURE 6 Light-grown mutant cell. Starch plate (*sp*) at the periphery of the pyrenoid (*p*). Note the wavy layered structure of the plate more clearly visible along its heavily stained margins. The repeat is  $\sim 50$  A and each dense band seems to be split lengthwise by a lighter line. Pyrenoid particles are marked *pp*, chloroplast ribosomes *cr*, and a granum *g*.  $\times 210,000$ .

FIGURE 7 Light-grown mutant cell. Small field at the periphery of the eyespot which in this case consists of two rows of dense granules (*eg*<sub>1</sub>, *eg*<sub>2</sub>) (in three dimensions, two plates). The plates are separated by a single chloroplast disc (*d*<sub>1</sub>); other discs appear in oblique section at *d*<sub>2</sub>. The chloroplast envelope consists of two membranes of different appearance: the outer one is thicker and has a well defined stratified structure; the inner one is thinner, less clearly stratified and, as such, more similar to the disc membrane. Areas of fusion of the two membranes are marked by arrows. The cell membrane (*mb*) shows clearly its stratified asymmetric structure with the outer leaflet denser and thicker than the inner one. Note that at the level of the eyespot the inner leaflet is backed by condensed cytoplasmic matrix which, in places, seems to fill the gap between the cell membrane and the chloroplast envelope. The cell wall is marked *w*.  $\times 180,000$ .



Each light- or dark-grown cell contains a single plastid shaped as a cup with a deeply festooned (lobated) rim (Figs. 2, 3, and 12). The shape is more regular in chyl than in chyd cells. The plastid is limited by an envelope comprised of two membranes frequently fused over a variable area (Fig. 7). The outer membrane of the envelope is  $\sim 75$  A thick and has the usual appearance of a symmetric unit membrane; the inner membrane is thinner ( $\sim 55$  A), often appears as a single dense band (Fig. 7) and is only in places resolved into a trilayered structure. As such, it is structurally similar to the membrane of the chloroplast discs. The space limited by the plastid envelope is occupied by a matrix which has a density comparable to, or in certain cases higher than, the surrounding cytoplasmic matrix.

Within the plastid matrix are located the following structures:

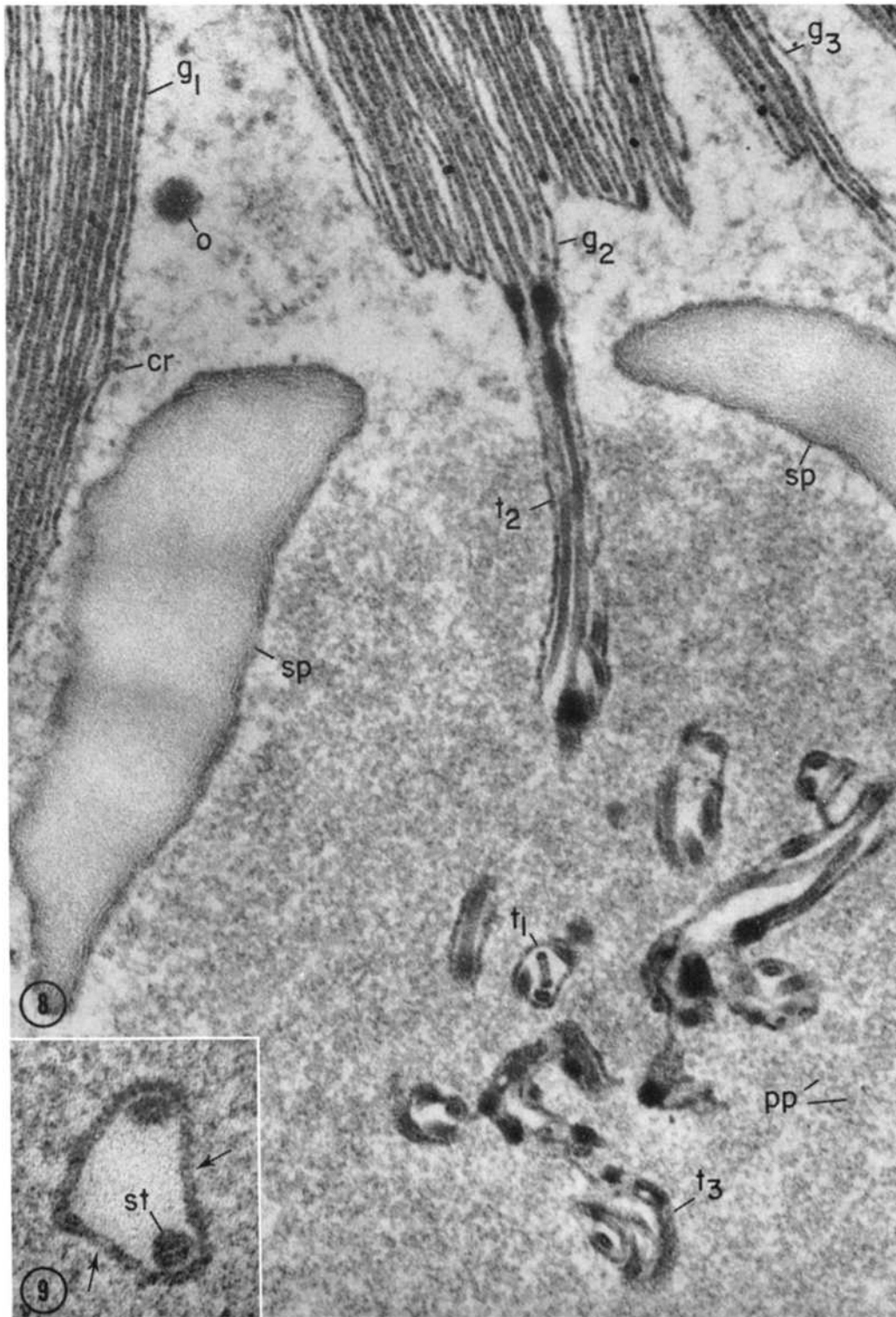
*a.* The pyrenoid, a polygonal-to-round body which measures 1.5–2.5  $\mu$  and is situated at the basal part of the plastid. It is built up of a tightly packed, dense granular material and a system of permeating tubules. At the periphery of the pyrenoid, these tubules are predominantly radially disposed, while in the center of the body they form a network (Figs. 3, 8, and 13). Normal sections show that each tubule is limited by a 55–60-A thick membrane, resolvable in places into three layers (Fig. 9) and contains in its lumen two to five (usually three to four) dense, peripheral bodies (Figs. 8 and 9). Favorable sections show that these bodies are tight, partly fused folds of the limiting membrane, and longitudinal sections indicate that these folds form inward protruding ridges of considerable but indeterminate length. In some places, the fold is detached from the limiting membrane and appears as a small excentric tubule within the

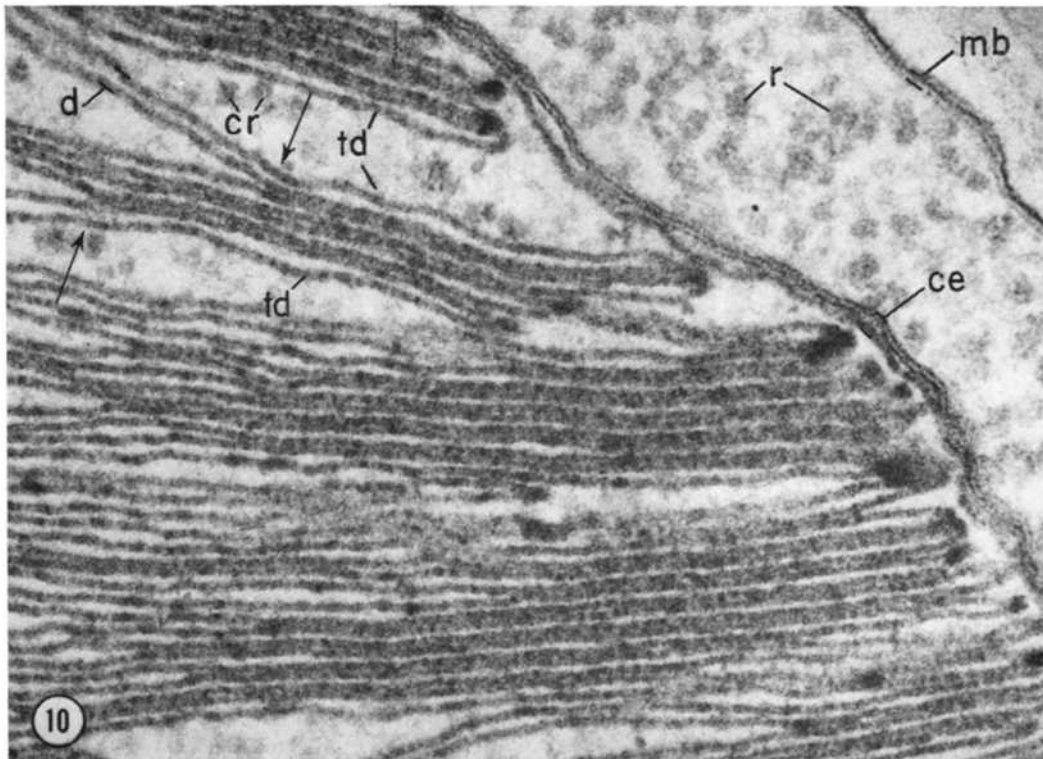
lumen of the tubular elements of the pyrenoid (Fig. 9). The infoldings are rare or absent in the central, usually narrow (diam: 300–500 A) tubules of the pyrenoid which are organized in networks, but are a constant feature of the wider (diam: 600–800 A), peripheral, radially oriented tubules. The latter extend beyond the pyrenoid and become continuous with the grana in chyl cells (Fig. 8) and with the residual tubular or cisternal elements of the plastid in chyd cells (Fig. 13). The folding pattern of the pyrenoid tubules is similar to that seen in the discs or thylakoids of many grana (see below). In fact, the tubular lumen is in continuity with the intradisc space, while the often-fused folds are continuous with the fused partitions of the grana (Fig. 8). The dense granular core of the pyrenoid is surrounded and clearly delineated from the rest of the plastid by starch plates of variable forms and sizes. In chyl cells in logarithmic growth, the plates are thin (0.1–0.2  $\mu$ ), flat, or biconcave, and usually confined to the immediate vicinity of the pyrenoid around which they form a discontinuous, spherical shell (Figs. 2, 3, and 8). The spaces in between the plates are filled with a light amorphous material through which pass the elements that connect the plastid discs with the tubular system of the pyrenoid. In dark-grown cells, the general arrangement is the same, but the plates increase in size to form round-shaped to irregular bodies. Moreover, similar bodies appear free in the matrix throughout the plastid (Figs. 12 and 13). The number of starch granules can increase considerably in chyd cells so that, in some cases, they practically fill up the plastid. The granules tend to stain more heavily at the periphery but are not bounded by a membrane. Often it is possible to resolve within the starch plates and granules, especially at their periphery, a periodic

---

FIGURE 8 Mutant cell grown in the light in batch type culture. The micrograph shows a sector of the pyrenoid, demonstrates the continuity of a pyrenoid tubule ( $t_2$ ) with a chloroplast granum ( $g_2$ ), and suggests that the ridges or infoldings of this tubule are in continuity with the fused membranes of the granular discs. The latter detail is obscured by a series of dense droplets of unknown significance which occur along the ridges. Other grana appear at  $g_1$  and  $g_3$ , and other pyrenoid tubules at  $t_1$  (cross-section) and  $t_3$  (oblique section). In this case, most of the pyrenoid tubules are of peripheral type, i.e., ridged and of relatively large caliber. Starch plates are marked *sp* and pyrenoid particles *pp*.  $\times 120,000$ .

FIGURE 9 shows at a higher magnification a pyrenoid tubule, to demonstrate the layered structure of the membrane (arrows) and the presence of at least one internal secondary tubule (*st*) presumably formed by a "detached" ridge.  $\times 200,000$ .





FIGURES 10 and 11 Mutant cells grown in the light in batch type culture. The micrographs compare the appearance of  $\text{OsO}_4$ -fixed grana (Fig. 10) with that of grana fixed in  $\text{OsO}_4$  and postfixed in  $\text{UO}_2$  acetate (Fig. 11). In the  $\text{OsO}_4$ -fixed specimen, the discs within each granum are closely apposed; their membranes are in contact although in places they still remain separated by a fine, discontinuous light line. Light intradisc spaces are generally visible and appear more distended in the terminal discs of the grana (*td*) and in intergranular discs (*d*).

In the  $\text{OsO}_4$ -fixed,  $\text{UO}_2$  acetate-postfixed specimen, a relatively heavy dense line ( $f$  = fusion line) is seen wherever the discs are apposed to one another in a granum. The intradisc space is collapsed over relatively large distances and in many areas is replaced by a dense line ( $f^1$ ) finer and less dense than the fusion line. Note the heavy  $\text{UO}_2$ -staining of ribosomes in both the cytoplasm and the chloroplast and the unchanged appearance (symmetrical) of the cell membrane in Fig. 11. In both figures the arrows point out the entrance of a disc or a group of discs into a granum, and the beginning of an ensuing fusion line.  $\times 190,000$ .

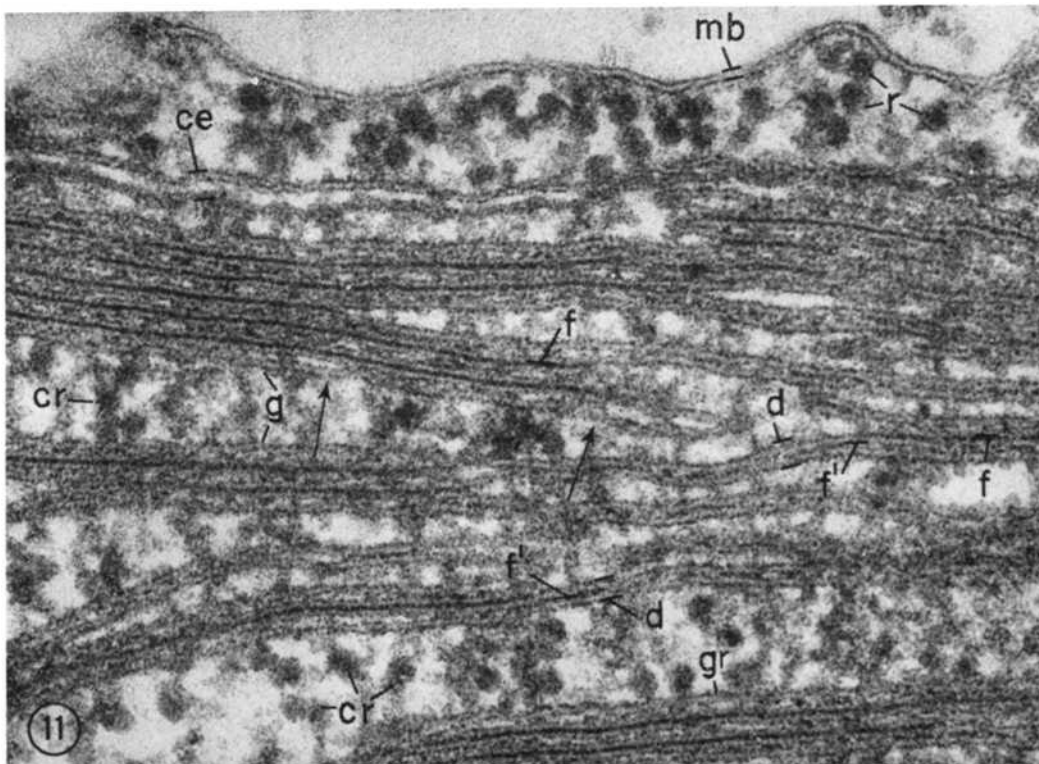
structure consisting of parallel or concentric layers, spaced at  $\sim 50 \text{ \AA}$  (Fig. 6).

*b.* The eyespot (stigma) is an array of polyhedral granules, each of about  $0.1 \mu$  diameter, arranged in rows (usually two to three) separated by one or two disc(s), and located immediately under the envelope, on one side of the plastid (Fig. 7). In grazing sections it reveals a close, regular, predominantly hexagonal packing of its constitutive granules. In dark-grown cells the degree of order is affected to a variable extent. Usually, the granules

are irregular in size and shape and appear scattered within the matrix of the plastid (Fig. 12).

*c.* The main difference between the chyl and chyd cells is found at the level of the intraplastid membranous system. In light-grown cells, this system consists of uniformly flattened discs (diam:  $0.6\text{--}1.0 \mu$ ) bounded by a membrane  $\sim 55 \text{ \AA}$  thick and assembled in stacks or grana containing from two to 20 fused discs (Figs. 2, 3, 10, 11). The detailed structure of the disc membrane is rather complex. It can be resolved in places into a typical





unit membrane. Its intermediate layer is rather dense (Figs. 10 and 11); moreover, there is a suggestion of periodicity normal to the plane of the membrane with a spacing of  $\approx 100$  Å. This periodicity is similar to that described in other chloroplasts (56, 57), is more evident within grana, and appears to be in phase in adjacent discs. Within grana the discs are fused, and in the plane of fusion a highly dense,  $\sim 25$ -Å-thick layer can be detected in specimens stained in block with uranyl acetate before dehydration (Figs. 10 and 11). In such specimens, the intradisc space is also frequently collapsed and replaced by another fusion layer thinner ( $\sim 20$ -Å) and less dense than that found in between fused discs (Fig. 11). The main fusion layer (line in sections) is reminiscent of detail described in  $\text{KMNO}_4$ -fixed grana of *Scenedesmus* and higher plant chloroplasts by Weier et al. (57). The grana are distributed throughout the entire plastid, with the exception of the pyrenoid region. They are usually oriented parallel to the chloroplast envelope, and are interconnected by single discs, pairs of discs, or groups of more than two discs common to two or more stacks (Figs. 2 and 3). The ratio of fused discs forming a granum (intragranar)

to the total number of discs (intra- + intergranar) in light-grown cells is in the range of 0.75 (Fig. 14 c). Pairing and fusion is usually seen between two apparently separate discs, but single discs are found which are bent at  $180^\circ$  upon themselves to form spurious pairs. The fold of a bent disc is occasionally found fused to a varied extent, the results being a minimal granum. Such appearances are especially evident during the formation of the disc system in the greening process when the discs are relatively small and are not yet tightly fused into grana (49).

In dark-grown mutant cells, only a varying amount of disc remnants occur and take the form of distended, irregular vesicles or short irregular, flattened, often fenestrated cisternae (Figs. 12 and 13). Bent, "V"-shaped cisternae are often seen (Fig. 12) and occasionally pairs of small, fused discs are still encountered, but, as it will be pointed out later, the ratio of the intragranar to total disc-remnant membranes is less than 0.2 (Fig. 14 c). The tubular system of the pyrenoid is still connected with such remnants (Fig. 13). The internal space of the vesicles and flattened cisternae appear

to be much lighter than the plastid matrix which surrounds them.

The aforementioned structures, i.e. discs, pyrenoid, starch plates or granules, and eyespot, are embedded within a matrix which occupies all the complementary chloroplast space. The matrix has a fine granular-to-fibrillar texture of a density comparable to that of the surrounding cytoplasm (Figs. 2 and 3).

Within the chloroplast matrix are scattered numerous ribosome-like particles. In specimens fixed in glutaraldehyde-Mg<sup>2+</sup> they appear to be smaller than the cytoplasmic ribosomes, having an average short axis of  $208 \pm 32$  Å and a long axis of  $266 \pm 32$  Å (Fig. 4). In OsO<sub>4</sub>-fixed specimens, chloroplast ribosomes are less well preserved and appear markedly smaller than cytoplasmic ribosomes (Figs. 3 and 10). A difference in dimensions between the two ribosomal populations is in agreement with the reported difference in their sedimentation coefficients (58–61).

The chloroplast matrix contains also a network of fine fibrils (~20–50 Å in width) more easily discerned in regions of low matrix density. The fibrils are similar in location and appearance to those considered by Ris and Plaut as chloroplast DNA fibrils (22).

#### *Enzymes in Dark- and Light-Grown Cells*

Since the chyd cells lack chlorophyll and chloroplast membranes, it was of interest to assay them for some of the enzymes involved in photosynthesis, particularly those involved in photosynthetic electron transport. The enzymes were compared on a per cell basis in the chyl and chyd cells grown for 6–7 days in batch cultures. Although the results

showed considerable variation from one cell batch to another,<sup>4</sup> they indicated that a number of chloroplast enzymes were still present in relatively high concentrations even in the absence of photosynthesis and the near absence of chlorophyll.

The photoreduction of DCI (Hill reaction) by homogenates of chyl cells proceeded at a rate of  $1.17 \pm .25$   $\mu\text{mole DCI}/\text{min}/\mu\text{g chlorophyll}$ , while the photoreduction rate of NADP was 4.3  $\mu\text{mole NADP}/\text{min}/\mu\text{g chlorophyll}$ . Photoreduction of NADP and oxygen evolution were not detectable in chyd cells. Both alkaline FDPase and NADP-linked G-3-P dehydrogenase were present in chyd cells, and their activities reached ~70% of those found in chyl cells (Table I). Ferredoxin-like activity was present in chyd cells at levels of 25–80% of that measured in chyl cells (Table I) while RuDP carboxylase activity in chyd cells amounted to 75–80% of that found in chyl cells (cf. following paper, 49). Cytochrome *f* was also detected in both chyd and chyl cells; the difference in absorbancy between 554 and 540  $m\mu$  was  $3.1 \times 10^{-4}$  OD units for chyd cells and  $7.0 \times 10^{-4}$  OD units for chyl cells tested at the same concentration and under the same conditions (Fig. 14 *b*), indicating this component was present in chyd cells at ~45% of the concentration found in chyl cells. A difference absorption spectrum during a greening process of chyd cells is shown in Fig. 15. We

<sup>4</sup>The wide variations in the levels of various enzymes (Table I) may be explained by the fact that these batch-grown cells were harvested either at the end of the logarithmic phase of growth or at the beginning of the stationary phase. Such variations were not found in cells grown in the semicontinuous culture apparatus (cf. Fig. 14).

---

FIGURE 12 General morphology of a mutant cell grown in the dark for five to six generations. Note the persistence of the chloroplast—represented in this transverse section by five profiles (*c*<sub>1</sub>–*c*<sub>5</sub>) of its lobes—but the marked decrease in the content of chloroplast discs. Only a few disc remnants (*d*) persist; some of them are bent in a “V” shape (*db*); very few are still paired (*dp*). Large starch granules (*sg*) fill a sizable part of the plastid. An extensively disorganized eyespot appears at *e*; note that in its immediate vicinity the frequency of disc remnants is higher.

Mitochondria, larger in size and with more cristae than in light-grown cells, are marked *m*. The cell has a large population of ribosomes both free (*r*<sub>1</sub>) and attached (*r*<sub>2</sub>); the latter are disposed in patterns among which double rows predominate. Irrespective of growth conditions (light or dark), the vacuoles (*v*) of the algal cells contain granules of inherently dense material (metaphosphate?) which frequently falls from the sections during cutting. This explains the “holes” seen in the vacuole of this figure as well as in the vacuole of Fig. 3.  $\times 32,000$ .



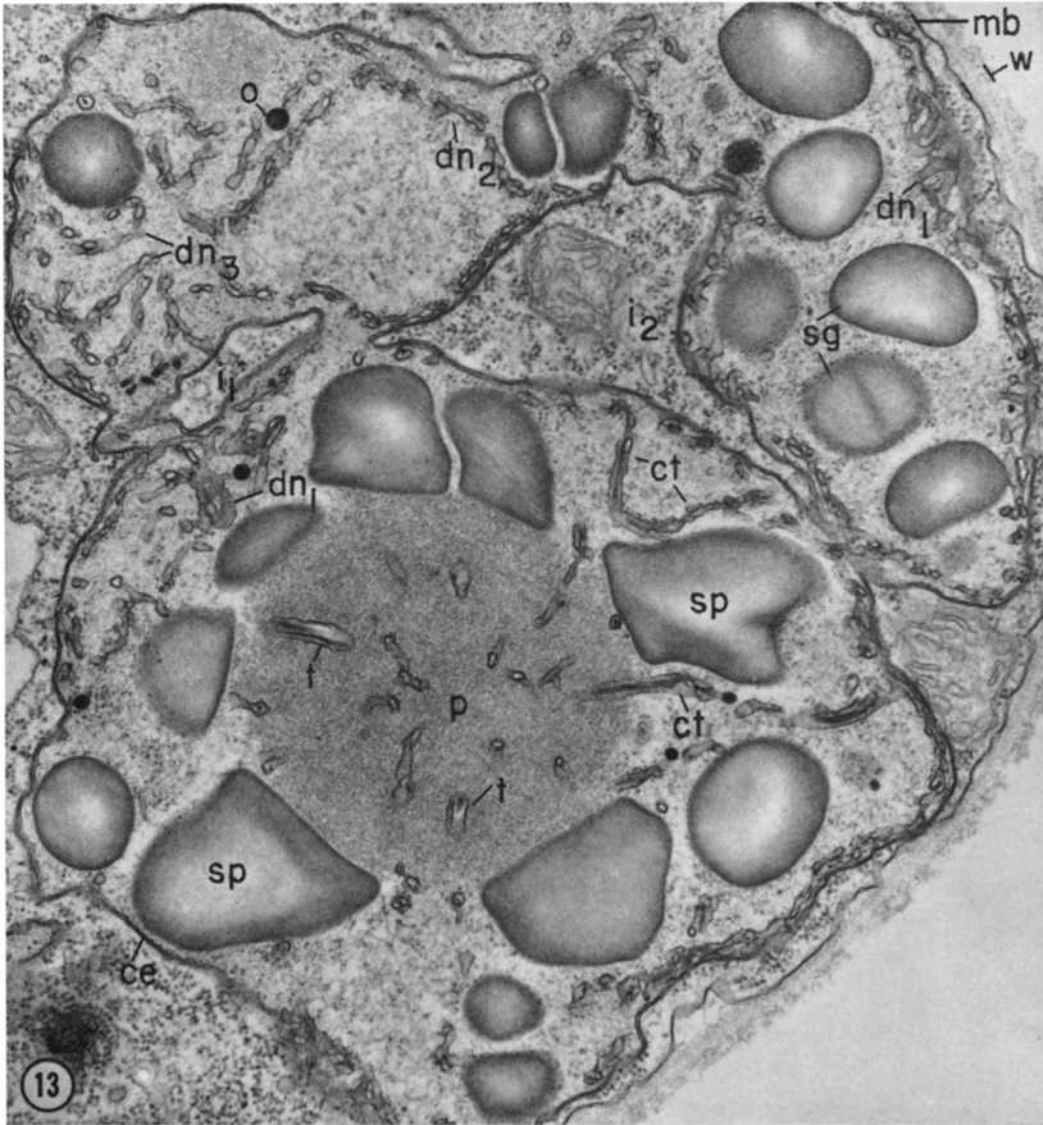


FIGURE 13 Relatively thick section through the posterior half of the plastid in a dark-grown cell. The irregular form of the plastid is apparent from the complicated outline of its profile which surrounds two cytoplasm "islands" ( $i_1$ ,  $i_2$ ). The pyrenoid appears at  $p$ , penetrated by tubules ( $t$ ) whose appearance changes from the periphery (folded or ridged tubules) to the center (simple tubules). Heavy starch plates ( $sp$ ) of irregular plane-convex shape surround the pyrenoid, and large starch granules ( $sg$ ) occur in the rest of the plastid. Disc remnants can be seen concentrated at the periphery of the plastid, immediately under the envelope, and appear to be organized in approximately planar networks that can be clearly visualized where the section is oblique to the plane of the network ( $dn_1$ ). This type of organization explains appearances seen in other parts of the plastid where the networks, cut normally, appear as linear series of distinct profiles ( $dn_2$ ), or as series of mixed elongated and circular profiles ( $dn_3$ ). Disc remnants are connected through folded or ridged tubules ( $ct$ ) to the tubular system of the pyrenoid.  $\times 30,000$ .

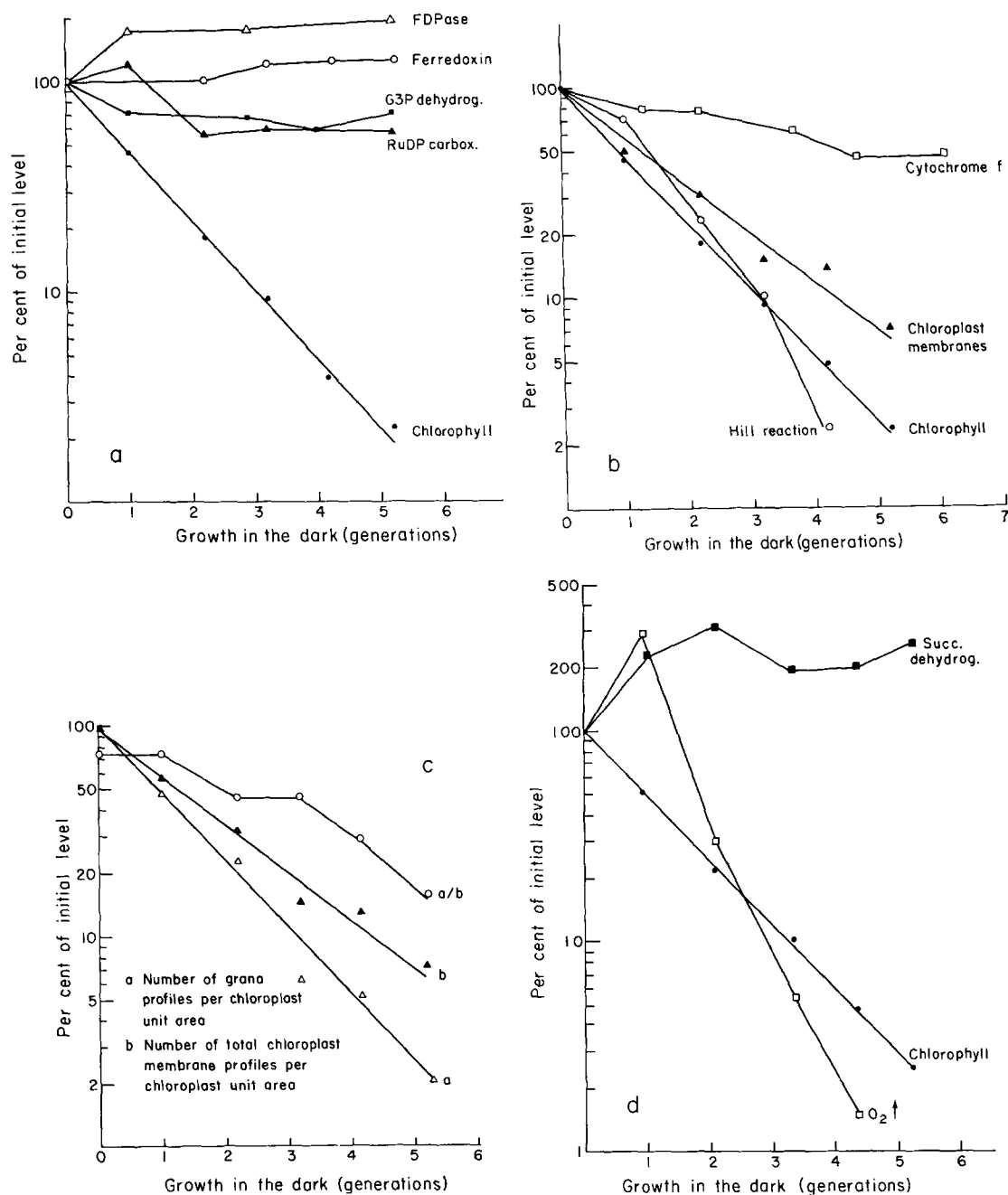


FIGURE 14 Concentration of chlorophyll, chloroplast membranes, and various enzymes in mutant cells as a function of number of generations of growth in the dark in a semicontinuous culture apparatus. The maximal cell concentration allowed before dilution was  $1.8 \times 10^6$  cells/ml. The generation time was 22 hr. The initial levels (100%) were as follows: (a) Chlorophyll,  $34 \mu\text{g}/10^7$  cells; FDPase, pH 8,  $0.33 \mu\text{mole Pi}/30 \text{ min}/10^7$  cells; RuDPCarboxylase,  $50.3 \text{ m}\mu\text{moles CO}_2\text{-fixed}/10 \text{ min}/10^7$  cells; ferredoxin,  $42 \text{ m}\mu\text{moles NADP-reduced}/\text{min}/10^9$  cells; G-3 P dehydrogenase,  $0.072 \mu\text{mole NADP reduced}/\text{min}/10^7$  cells. (b) Hill reaction,  $0.088 \mu\text{mole DCI reduced}/\text{min}/10^7$  cells; cytochrome *f*,  $2 \times 10^{-3} \text{ OD}/10^7$  cells; chloroplast membranes index,  $1.9 \text{ intersections}/\text{cm}^2$  for a total of 2217 membrane profiles counted. (c) Grana fusion lines index,  $0.68/\text{cm}^2$ ; ratio of grana fusion lines index to total chloroplast membrane index (%). (d) Succinic dehydrogenase,  $1.5 \mu\text{moles}/10 \text{ min}/10^8$  cells; oxygen evolution,  $4.2 \mu\text{moles}/10 \text{ min}/10^8$  cells.

TABLE I

## Enzyme Activities in Green and Yellow Mutant Cells

Assays were performed as described in Methods. The number of homogenized cells used for enzyme assays was:  $4-8 \times 10^7$  for the FDPase;  $1-2 \times 10^6$  for the NADP-linked G-3-P dehydrogenase; and  $8 \times 10^6$  to  $2 \times 10^7$  for ferredoxin activity. Dark-grown cells were harvested after 6-7 days of batch-type growth.

Enzyme act.	Light-grown cells (chyl)	Dark-grown cells (chyd)
ph 8.8 FDPase	0.21 $\mu$ moles Pi/30 min/ $10^7$ cells (Av. of 7 exps.; range, 0.15-0.39)	0.16 $\mu$ moles Pi/30 min/ $10^7$ cells (Av. of 4 exps.; range, 0.10-0.24)
NADP-linked G-3-P dehydrogenase	0.147 $\mu$ moles NADPH/1 min/ $10^7$ cells (Av. of 4 exps.; range, 0.104-0.214)	0.107 $\mu$ moles NADPH/1 min/ $10^7$ cells (Av. of 4 exps.; range, 0.102-0.121)
Ferredoxin activity	Exp. 1. 163 $m\mu$ moles NADPH/1 min/ $10^9$ cells* Exp. 2. 92 $m\mu$ moles NADPH/1 min/ $10^9$ cells§	Exp. 1. 38 $m\mu$ moles NADPH/1 min/ $10^9$ cells† Exp. 2. 79 $m\mu$ moles NADPH/1 min/ $10^9$ cells

\* 20.5  $m\mu$ moles NADPH/1 min/mg protein

† 13.2

§ 52.8

|| 64.8

have no explanation for the significance of the variable extent of decrease in the amount of these enzymes in the chyd cells; nevertheless, the main point is that they are present in significant amounts in these cells.

When chyd cells were incubated in the dark in the presence of acetate- $^{14}$ C, radioactive carbon was incorporated into mono- and digalactosylglycerol lipids as well as in sulfolipid and phospholipid fractions. The general pattern of the spots on the radioautograms was similar to that of the lipids extracted from chyl cells, thus indicating the active presence in chyd cells of the enzyme systems involved in lipid synthesis (Fig. 16). Initially, the rates in the dark were similar to those in the light, then tended to fall off (cf. following paper, 49).

The mutant cells grown in the dark continued to synthesize carotenoids, as indicated by the absorption spectra of 80% acetone extracts of chyd cells. They also retained the ability to synthesize chlorophyll when exposed to light at rates comparable to those of chyl cells but, under standard conditions of testing, the synthesis was usually resumed only after a lag period of 1.5-4.5 hr (Fig. 17). Apparently, the length of this lag period was correlated to the number of cell generations in the dark. However, it was found that the condition of

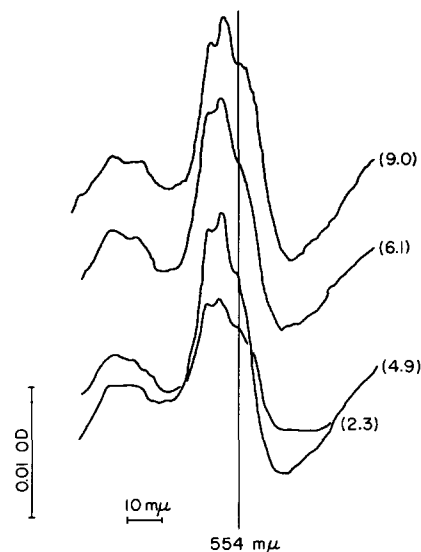


FIGURE 15 Difference absorption spectra of dark-grown mutant cells during a greening process. Extracts from  $5 \times 10^7$  cells for each sample were suspended in 0.1 M phosphate buffer, pH 7.4, and frozen in a lucite cell in liquid nitrogen. The difference spectra of their reduced ( $\text{Na}_2\text{S}_2\text{O}_4$ ) versus oxidized (ferricyanide) cytochrome *f* were recorded with a split-beam spectrophotometer. Numbers in parenthesis are chlorophyll concentrations ( $\mu\text{g}/10^7$  cells).

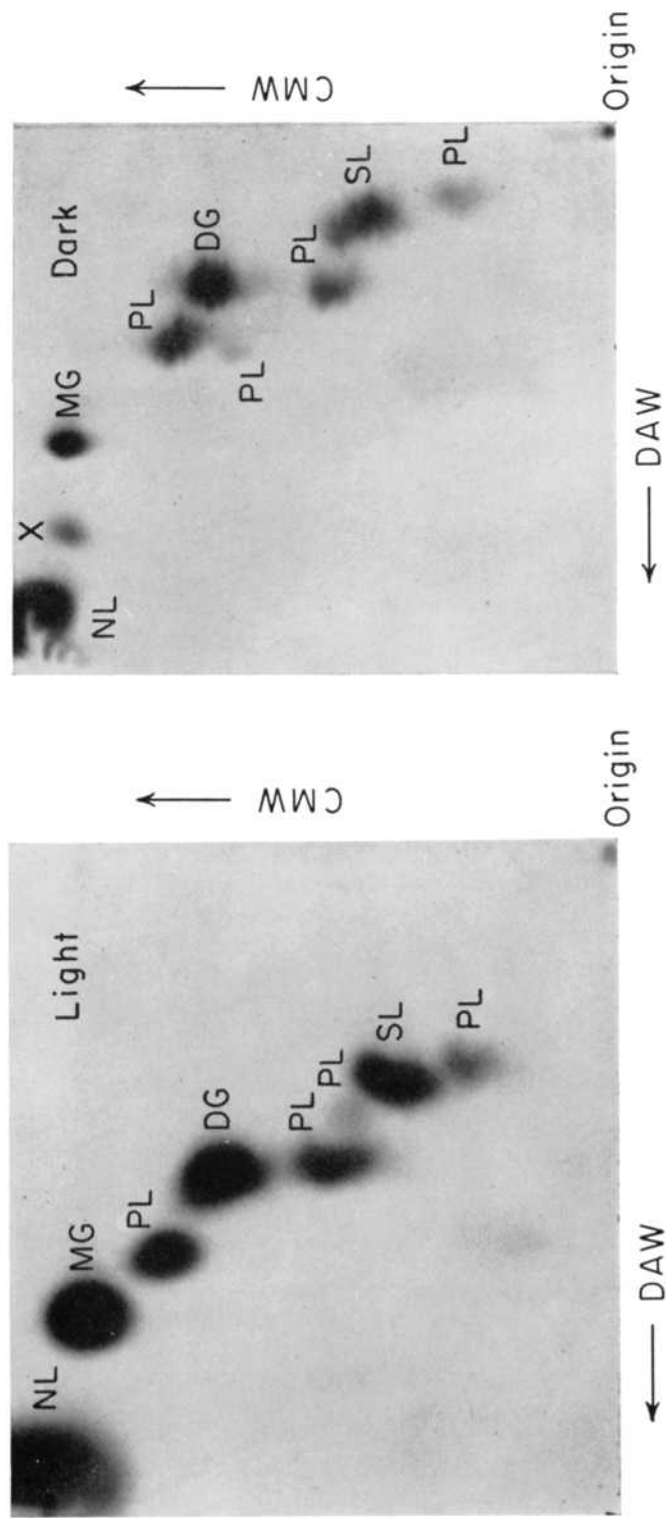


FIGURE 16 Radioautogram of a chromatogram of  $^{14}\text{C}$ -labeled, nondeacylated lipid extracts from chyd cells incubated in the dark or light with acetate- $^{14}\text{C}$ . Chyd cells were incubated at a final concentration of  $1.1 \times 10^7$  cells/ml in the usual growth medium, in which acetate- $^{14}\text{C}$  was replaced by uniformly labeled acetate- $^{14}\text{C}$  ( $9 \mu\text{c}/\mu\text{mole}$ ). Incubation was for 5.5 hr in the dark or light. For each sample, an extract from  $4.4 \times 10^7$  cells was used. Its total radioactivity was  $9.8 \times 10^5$  cpm for light-exposed cells, and  $3.7 \times 10^6$  for cells maintained in the dark. Initial chlorophyll concentration was  $0.66 \mu\text{g}/10^7$  cells maintained in the dark; it increased to  $17 \mu\text{g}/10^7$  cells in the light-exposed sample.

*MG*, monogalactosyl glyceride; *DG*, digalactosyl glyceride; *PL*, phospholipids; *SL*, sulfolipid; *NL*, neutral lipid; *X*, unknown; *DAW*, disobutyl ketone-acetic acid-water; *CMW*, chloroform-methanol-water.

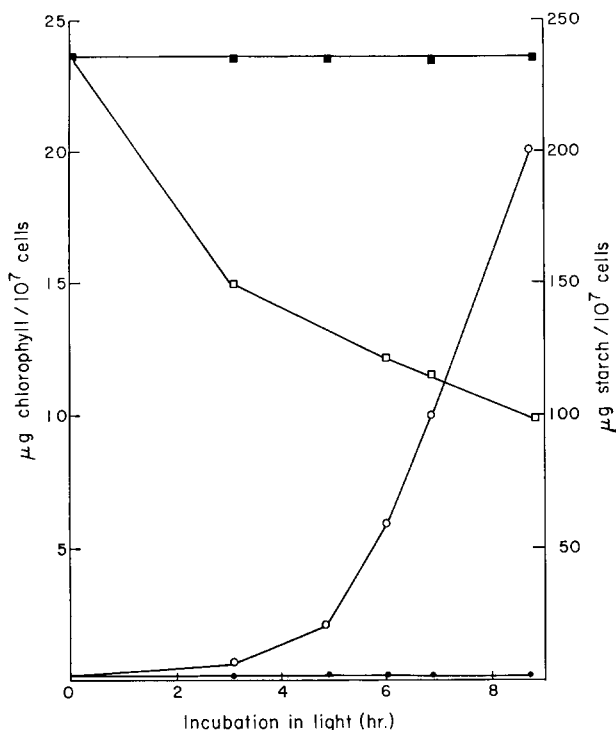


FIGURE 17 Kinetics of chlorophyll synthesis and starch degradation by chyd cells exposed to light. Cells were grown in batch culture for 7 days and exposed to light in fresh medium at an initial concentration of  $8 \times 10^6$  cells/ml. Chlorophyll in the light:  $\circ$ — $\circ$ ; dark control:  $\bullet$ — $\bullet$ ; starch in the light:  $\square$ — $\square$ ; dark control:  $\blacksquare$ — $\blacksquare$ .

incubation in terms of cell concentration, surface-to-volume ratio of the cell suspension, and light intensity influenced markedly the length of the lag period, which under optimal conditions could be reduced from  $\sim 4.5$  hr to  $\sim 35$  min (Figs. 18 *a* and *b*).

Although the mutant cells could accumulate large amounts of starch when grown in the dark, they apparently still contained the enzymic apparatus necessary for its degradation. This process, however, seemingly had to be initiated by exposure to light (Fig. 17), and continued at an almost constant rate without showing a lag period. The rate of degradation was not correlated with the number of generations of growth in the dark and was about  $35 \pm 5$   $\mu\text{g}$  starch degraded/hour/ $10^7$  cells.

#### The Degreening Process

The phenotypic transformation of the light-grown mutant into a typical chyd cell involved a drastic reduction in chlorophyll content ( $\sim 97\%$ ) and in the chloroplast disc system accompanied by a virtual disappearance of photosynthetic activity, but a much less extensive decrease in the activity of various enzymes associated with the chloroplast (Table I). The above findings relate to an analysis of the mutant grown 5–8 days in batch cultures.

The observed changes could result from: (*a*) a reduction in the synthetic rate or a complete cessation of synthesis, (*b*) an active degradation process of the compounds involved, or (*c*) a combination of both processes. Reduction rates equal to growth rates would suggest a complete cessation of synthesis; higher reduction rates would imply dilution and degradation, while lower reduction rates would suggest that dilution, reduced synthesis, and small or negligible degradation were concurrently occurring. Thus, it is possible to gain insight into the events involved in the transition of chyl into chyd cells by following the concentrations of various cellular components during logarithmic growth of the mutant after placing it in the dark.

The cells were “degreened” as described under Methods, and the changes in morphology of the cells, as well as pigment concentration and enzymatic activities, were followed with each cell division. The results are shown in Figs. 14 *a–d*. It is evident that the decay rates of the activities of various soluble enzymes and the concentration of cytochrome *f* differ markedly from those of photosynthetic activity and chlorophyll concentration. The data suggest that chlorophyll synthesis stopped completely in the dark and the pigment was diluted through cell division with a half-life of 0.98



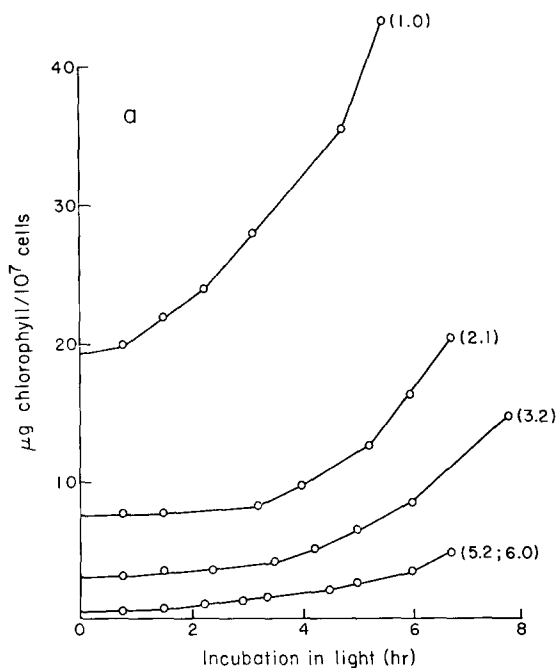


FIGURE 18 Chlorophyll synthesis in mutant cells exposed to light after a variable number of generations of growth in the dark in a semicontinuous culture apparatus (maximal concentration before dilution of  $2 \times 10^6$  cells/ml). The various cell batches have decreasing initial concentrations of chlorophyll as a consequence of growth in the dark for an increasing number of generations. Fig. 18 *a* Cells were washed in chilled growth medium, resuspended in fresh medium at a final concentration of  $\sim 2 \times 10^6$  cells/ml in a final volume of 130 ml in 500-ml Erlenmeyer flask and incubated in light ( $\sim 700$  ftc). Numbers in parentheses represent number of generations of growth in the dark.

generation. The Hill reaction has an initial half-life (after one division) of 1.5 generations, which drops during subsequent divisions to a value of 0.7 generation. The oxygen evolution increased almost three times at the first generation and decreased during the following divisions with an approximate half-life of 0.4 generation. At the same time, succinate dehydrogenase activity, which was assayed as a measure of mitochondrial activity, increased about three times at the first generation and changed only slightly during following divisions in the dark. Of more import, various soluble chloroplast-associated enzymes and cytochrome *f* continue to be synthesized in the dark (Figs. 14 *a* and *b*). After various changes in concentrations during the first or second division, they reach a

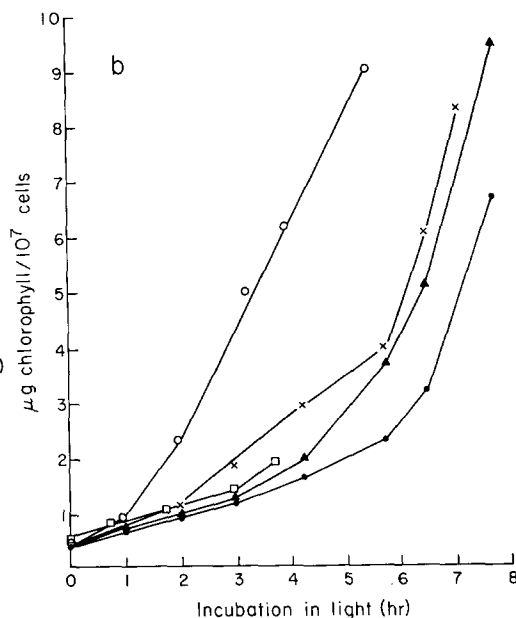


Fig. 18 *b* Cells from the 6th generation were exposed to light under different conditions. 1,  $\circ$ — $\circ$ , non-washed, transferred directly in the growth vessel from dark to light. Cell concentration  $1.3 \times 10^6$ /ml; 2.0 l,  $\sim 700$  ftc. 2,  $\times$ — $\times$ , cells washed and resuspended in fresh medium,  $1.75 \times 10^6$  cells/ml, 130 ml,  $\sim 700$  ftc. 3,  $\bullet$ — $\bullet$ , same as (2), but  $5.25 \times 10^6$  cells/ml. 4,  $\blacktriangle$ — $\blacktriangle$ , same as (2), but 250 ftc. 5,  $\square$ — $\square$ , same as (2), but  $2.3 \times 10^6$  cells/ml; cells kept in ice for 3 hr.

steady-state level which varies for the different enzymes tested from  $\sim +50\%$  to  $-50\%$  of the chl level.

The photoreduction of NADP (in the presence of excess added ferredoxin) decreases, following closely the chlorophyll pattern for the first two generations. This activity could not be measured after the second generation since the homogenate concentration required to test the activity was too high and obscured the reaction by its turbidity.

At the morphological level, progressive changes were observed only in the chloroplast (Figs. 19 and 20). The total amount of membranous material was reduced at each generation (Fig. 14 *c*). The length of membranes fused into grana diminished, as well as the number of discs in a stack. By the third generation the discs became unfolded and swollen, and the stacks were dispersed into separate flattened sacs or vesicles. This process continued during the following generation (Fig. 20) so

that only a few small, irregularly shaped vesicles and relatively short flattened sacs were present in the chloroplast after five to six generations (Figs. 12 and 13). Typical fusion of adjacent discs into grana was still occasionally observed up to the fourth generation of growth in the dark (Fig. 20). The accumulation of starch within the chloroplast was evident already at the second generation. The extent of disorganization of the eyespot globules was variable rather than progressive. No apparent change was observed in the structure of the pyrenoid besides a marked increase in size of the starch plates around its periphery. The network of the pyrenoid tubules and their connection with disc remnants was preserved throughout the duration of the experiment: six to seven generations grown in the dark.

#### DISCUSSION

The growth characteristics of the mutant used here are identical to those described for the wild type by Sager and Granick (31), and close to those of a similar mutant described by Hudock et al. (62, 63).

The morphological appearance of this mutant in liquid cultures was sufficiently homogeneous to justify normalization of biochemical data to cell number, since only a single chloroplast, containing one pyrenoid body, and only a single nucleus were present per cell.<sup>5</sup> The morphology of the light-

<sup>5</sup> Whenever dividing cells were observed in sections, they had only one nucleus for each daughter cell, and in such orientation and dimensions as to exclude the possibility that multinucleate cells were present, as previously indicated for this genus by Sueoka (64), and Buffaloe (65). It is possible that the occurrence of multinucleate cells as reported by these authors was at least partially due to their experimental conditions, since both used agar-grown cultures. Jacobson (66), who followed divisions immediately after transfer from agar to liquid cultures, found that 85% of the population was uninucleate, only 6% binucleate, with the remaining showing four to eight nuclei. Possible

grown mutant is practically indistinguishable from the wild type, which was described and discussed in detail by Sager and Palade (69), and very similar to the  $y^-$  mutant described by Hudock et al. (62, 63), as far as one can judge from the few micrographs published by these authors.

The dark-grown mutant progressively loses only the lamellar system of the chloroplast and acquires the typical "chyd" form within five to six generations. Thus at the morphological level, the dark-grown mutant still possesses a recognizable, partly differentiated plastid. Apparently similar results were obtained with dark-grown *Euglena* by Ben-Shaul et al. (70). However, wild type *Euglena* differs from the mutant *Chlamydomonas* in one basic aspect. In the former case, the extent of plastid dedifferentiation is greater and the chloroplast degenerates to the status of a proplastid. Not only the lamellar system disappears, but also the pyrenoids and many of the enzymes associated with the photosynthetic apparatus, as will be pointed out later.

During the degreening process there is relatively close, but not strict, association between the levels of chlorophyll, chloroplast lamellar systems, and photosynthetic activity. From the slopes of the curves relating chlorophyll content to generation time, it can be said that chlorophyll is not synthesized in the dark but diluted out by division. However, the half-life of the membranous phase of the chloroplasts was  $\sim 1.3$  generations (as compared to 1.7 generations in *Euglena*, 70), indicating that membrane synthesis occurs in the dark although at a low rate. Photosynthetic activity, as judged by the Hill reaction and  $O_2$  evolution, also did not follow exactly the change in the chlorophyll content. In the first generation, the Hill reaction was

difficulties in estimating the number of nuclei per cell intrinsic to these methods had already been mentioned by Jacobson et al. (67) and Kates and Jones (68).

---

FIGURE 19 Changes in the morphology of the chloroplast during a degreening process in which light-grown mutant cells were allowed to grow in the dark for three generations in the semicontinuous culture apparatus described under Methods. Chlorophyll content at the time of fixation:  $3.4 \mu g/10^7$  cells. Note the reduction in number and size of grana ( $g_1$ ,  $g_2$ ), many of which are reduced to pairs of short, fused discs ( $g_2$ ); note also the increase in number and size of starch granules ( $sg$ ) and the decrease in the frequency of ribosome-like particles ( $cr$ ) in the chloroplast matrix. A fused outfolding of the outer membrane of the chloroplast envelope is marked  $x$ .  $\times 100,000$ .



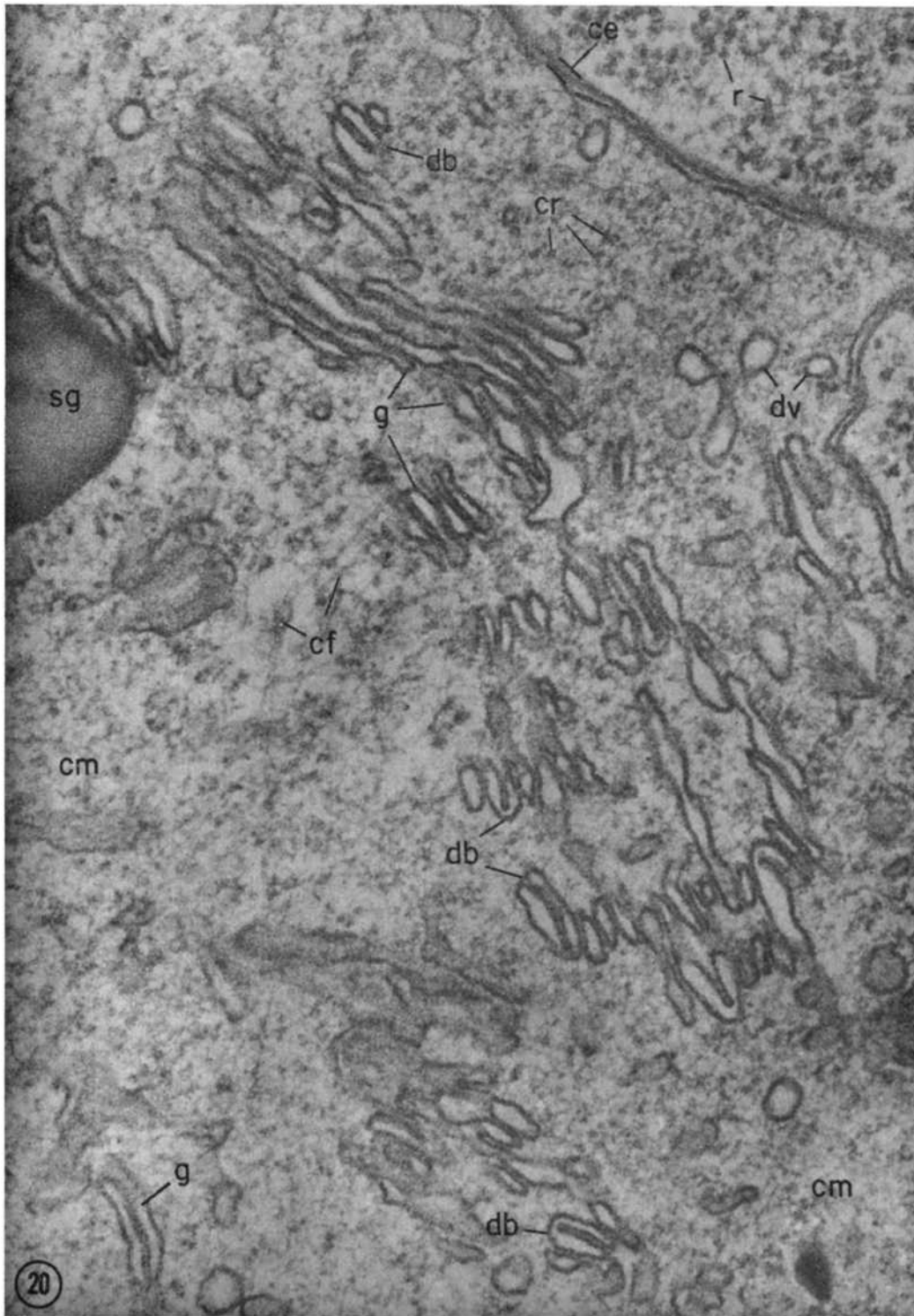


FIGURE 20 Mutant cell grown in the dark for four generations. Chlorophyll content at the time of fixation:  $1.5 \mu\text{g}/10^7$  cells. Further reduction in the number and size of grana (*g*) and discs has occurred. Many discs have been changed into isolated, irregular vesicles or tubules (*dv*) some of which are folded over and fused (*db*) into miniature or minimal grana. The ribosome (*cr*) population of the chloroplast is sparse (compare with the ribosome population of the cytoplasm (*r*)). Fine fibrillar elements (*cf*)—possibly DNA—appear in the chloroplast matrix.  $\times 90,000$ .

reduced (per cell) only to 60–80% (in different experiments) of the initial value, while oxygen evolution increased three-fold. A tentative explanation could be that light-grown cells contained an excess of nonactive chlorophyll which would become active during growth in the dark, possibly by inclusion in the small amount of membranes formed during this time. The per cent of fused or granar membranes also did not change during the first generation, in agreement with such an explanation, if one assumes that chlorophyll is more concentrated in the granar region than in the intergranar sections of the discs (71). In the following generations, the photosynthetic activity dropped faster than the chlorophyll content; we have no explanation for this result at present.

The wild type of *Chlamydomonas* is able to synthesize chlorophyll in the dark (62, 30; also this work, not shown), thus apparently differing from some green plants in its ability enzymatically to hydrogenate the chlorophyll precursors. Whether chlorophyll synthesis occurs in this organism along the scheme proposed by Granick (72) or by the one proposed by Wolff and Price (73) is not clear. In mutant strains of *Chlamydomonas*, the hydrogenating enzyme is presumably absent, for protochlorophyll (30) or protochlorophyllide is apparently accumulated in the dark.

The kinetics of chlorophyll synthesis by chyd cells exposed to light differ from those described for higher plants. The lag period is not preceded by a burst of synthesis as in higher plants (11), indicating that the amount of accumulated protochlorophyll is low. The synthesis in the linear phase after the lag period proceeds at a rate of  $4.0 \pm 0.4 \mu\text{g chlorophyll}/10^7 \text{ cells/hour}$  under the standard conditions described above, as compared with  $3.3 \pm 0.3 \mu\text{g}/10^7 \text{ cells/hour}$  for cells growing under continuous illumination, as calculated from the ratio chlorophyll/cell/division time in logarithmic phase. Thus, a normal and fully efficient apparatus for chlorophyll synthesis is present in chyd cells after 3.5–4.5 hr of illumination. This apparatus seems to be present even before illumination, as is apparent from the following considerations. If the concentrations of synthetic enzymes were diluted by division in the dark, a 50-fold dilution would be expected after six generations. If the “lag” phase of chlorophyll synthesis were due to a replenishment of the synthetic apparatus rather than to its activation, one would expect the length of the lag phase to increase proportionally

to the number of generations grown in the dark. Under the same conditions of illumination and cell concentration, cells show lags of  $\sim 45 \text{ min}$ ,  $\sim 3.5 \text{ hr}$ , and  $\sim 4 \text{ hr}$  one, two to five generations, and six generations in the dark, respectively. Thus the lag increases four times over a period of growth in the dark which would allow a dilution greater than 50-fold. Moreover, the lag for the six-generation dark-grown cells could be reduced to less than 1 hr under proper experimental conditions. The rate of chlorophyll synthesis before the linear rate is reached is not significantly increased by incubating the cells in the dark after short exposures to light, as expected if synthesis of the corresponding enzymes were induced by light; furthermore, upon reexposure to light, chlorophyll synthesis is resumed at a rate equal to that attained during the previous illumination (49). It seems thus possible to conclude that the synthetic apparatus for chlorophyll synthesis is not significantly diluted in mutant cells grown in the dark.

The RuDP carboxylase, G-3-P NADP-linked dehydrogenase, FDPase, ferredoxin, photosynthetic cytochromes, and PPN reductase are known to be located in plant chloroplasts (74–76), while cytochrome *f* was localized in plant chloroplasts by Hill and Bonner (44) and James and Leech (76). Cytochrome *f* is found in wild type *Chlamydomonas reinhardtii* (77) while ferredoxin and NADP photo-reductase are present in the wild type and mutants of *Chlamydomonas* (78). RuDP carboxylase was found to be present in both wild type and a similar mutant of *Chlamydomonas* (78, 62). A type-*c* cytochrome (79) and a cytochrome *b<sub>6</sub>* (80) were located in the chloroplast of light-grown *Euglena*. Of these enzymes, only cytochrome *f* and the PPN reductase are thought to be, by their very function, closely associated with the disc system, although cytochrome *f* can be easily solubilized and purified (81). The other soluble constituents may be regarded as markers for the matrix of the chloroplast; these were found to be present in the light-grown mutant at levels close to, or similar to those reported for the wild type and other mutants (62, 77, 78). When grown in the dark, chyd cells exhibit levels of these presumably chloroplast-matrix enzymes of  $\pm 50\%$  of the normal chyl cells. Since a dilution of  $\sim 50$ -fold can be expected, the presence of these enzymes in chyd cells implies that they continue to be synthesized in the dark.

The finding that cytochrome *f* was also present in chyd cells in which only trace amounts of disc

remnants were observed, suggests that in these cells the cytochrome is located in the matrix and becomes more closely associated with, or incorporated within the membranes once these are formed. Cytochrome *f* was also reported to be present in etiolated mung bean leaf and to be located in the plastids (45).

During growth in the dark, the mutant retains the ability to synthesize the lipids associated with the chloroplast lamellar system, as seen from incorporation of acetate into galactolipids and sulfolipid fractions. However, it is difficult to estimate the activity levels of these enzymes from the initial rates of incorporation in the light because of possible dilution of the labeled acetate with <sup>12</sup>C metabolites derived from the starch whose degradation is induced by light. It might be added that at least part of the enzymes responsible for chlorophyll synthesis and starch metabolism, as well as lipid synthesis, are also located in the chloroplast (75, 82).

Kinetics of starch solubilization suggest that the enzymic system responsible for this reaction is present in a "latent" form in the chyd cells and becomes fully activated as soon as cells are exposed to light. For, if these enzymes were to be synthesized by a light-induced process repressible in the dark, one would expect a dilution of these enzymes proportional to the number of cell generations in the dark. The initial reaction rates, however, were found to be constant and independent of the initial chlorophyll level (i.e. number of generations in the dark). This finding also implies that the degradation is not simply mediated by an immediate product of chlorophyll activity in the light.

In contrast to our results with the *y-1* mutant and those of Hudock et al. (62, 63) with the similar, if not identical *y<sup>-</sup>* mutant, the NADP-linked G-3-P dehydrogenase was reported to be very low in dark-grown *Euglena* and to increase in parallel to chlorophyll synthesis after illumination (83). This enzyme was reported to be formed during photomorphogenesis in higher plants (84), but also after illumination with red light in the ab-

sence of chlorophyll formation (85), apparently the induction of its synthesis being mediated by the phytochrome system. In some higher plants, RuDP carboxylase also appears to be induced during chloroplast formation (86). Photosynthetic cytochromes are absent in dark-grown *Euglena* (79). Also, the proplastids of this organism lack at least three soluble antigens which are sequentially induced during chloroplast formation (87). Thus, all the above proteins which appear to be formed during the differentiation and development of a proplastid into a chloroplast are present in relatively high concentrations in the dark-grown mutant of *Chlamydomonas*. It is, therefore, possible to consider the chyd mutant as having a partially differentiated plastid or half-differentiated "chloroplast" lacking only the discs and grana system, but containing the enzymes required for the synthesis of the molecular components of these structures (with the exception of chlorophyll). These components are synthesized and assembled into active structures, i.e. discs and grana, once chlorophyll becomes available during the greening process. In the following paper, it is proposed to analyze the physiology and morphology of this process in more detail.

We would like to thank Dr. Ruth Sager, Department of Biological Sciences, Hunter College, New York, for the stock culture of the *y-1 Chlamydomonas reinhardtii* mutant, and for advice on its cultivation. We would also like to thank Misses Mary Ledoux and Louise Evans for technical help, and Dr. Walter Bonner, Johnson Foundation, University of Pennsylvania, for aid in the determination of cytochrome *f* in his laboratory.

A part of this paper was presented at the Annual Meeting of the Federation of American Societies for Experimental Biology, Atlantic City, N. J. April, 1966 (88).

The work was supported by United States Public Health Service Grant No. 1-RO1 HD-01689 to Dr. Siekevitz.

Received for publication 10 April 1967; revision accepted 1 August 1967.

#### REFERENCES

1. LINNANE, A. W., E. VITOLS, and P. G. NOWLAND. 1962. *J. Cell Biol.* 13:345.
2. LUCK, D. J. L. 1963. *J. Cell Biol.* 16:483.
3. LUCK, D. J. L. 1965. *J. Cell Biol.* 24:461.
4. WALLACE, D. G., and A. W. LINNANE. 1964. *Nature.* 201:1191.
5. EPSTEIN, H. T., and J. A. SCHIFF. 1961. *J. Protozool.* 8:427.
6. MEGO, J. I., and A. T. JAGENDORF. 1961. *Biochim. Biophys. Acta.* 53:237.
7. BUTLER, W. L. 1961. *Arch. Biochem. Biophys.* 92:287.

8. GIBOR, A., and S. GRANICK. 1962. *J. Protozool.* **2**:327.
9. GRANICK, S. 1963. *Cytodifferential and Macromolecular Synthesis*. Academic Press Inc., New York. 144.
10. APP, A. A., and A. T. JAGENDORF. 1963. *J. Protozool.* **10**:340.
11. EILAM, Y., and S. KLEIN. 1962. *J. Cell Biol.* **14**:169.
12. STERN, A. I., H. T. EPSTEIN, and J. A. SCHIFF. 1964. *Plant Physiol.* **39**:226.
13. ISHIKAWA, I. S., and E. HASE. 1964. *Plant and Cell Physiol.* **5**:227.
14. AOKI, S., J. K. MATSUBARA, and E. HASE. 1965. *Plant and Cell Physiol.* **6**:475.
15. AOKI, S., M. MATSUKA, and E. HASE. 1965. *Plant and Cell Physiol.* **6**:487.
16. KAHN, A., and D. VON WETTSTEIN. 1963. *Photochem. Photobiol.* **2**:83.
17. KLEIN, S., G. BRYAN, and L. BOGORAD. 1964. *J. Cell Biol.* **22**:433.
18. BEN-SHAUL, Y., J. A. SCHIFF, and H. T. EPSTEIN. 1964. *Plant Physiol.* **39**:231.
19. GUNNING, B. E. S. 1965. *Protoplasma.* **60**:111.
20. GIBOR, A., and S. GRANICK. 1964. *Science.* **145**:3635.
21. SCHIFF, J. A., and H. T. EPSTEIN. 1965. In *Reproduction: Molecular, Cellular and Subcellular*. M. Locke, editor. Academic Press Inc., New York. 131.
22. RIS, H., and W. PLAUT. 1962. *J. Cell Biol.* **13**:383.
23. CHUN, E. H. L., M. H. VAUGHAN, JR., and A. RICH. 1963. *J. Mol. Biol.* **7**:130.
24. SAGER, R., and M. R. ISHIDA. 1963. *Proc. Natl. Acad. Sci. U. S.* **50**:725.
25. LEFF, J., M. MANDEL, H. T. EPSTEIN, and J. A. SCHIFF. 1963. *Biochem. Biophys. Res. Commun.* **13**:126.
26. SAGER, R. 1955. *Genetics.* **40**:476.
27. SAGER, R. 1962. *Genetics.* **47**:982.
28. SAGER, R., and Y. TSUBO. 1962. *Arch. Mikrobiol.* **42**:159.
29. SAGER, R., and Z. RAMANIS. 1963. *Proc. Natl. Acad. Sci. U. S.* **50**:260.
30. SAGER, R. 1961. *Carnegie Inst. Washington Yearbook.* **60**:374.
31. SAGER, R., and S. GRANICK. 1953. *Ann. N.Y. Acad. Sci.* **56**:831.
32. MILNER, H. W., N. S. LAWRENCE, and C. S. FRENCH. 1950. *Science.* **111**:633.
33. PRATT, R. 1963. *Am. J. Botany.* **30**:626.
34. BERNATH, P., and T. P. SINGER. 1962. *Methods in Enzymology*. S. P. Colowick and N. O. Kaplan, editors. Academic Press Inc., New York. 5:597.
35. RACKER, E., and E. A. R. SCHROEDER. 1958. *Arch. Biochem. Biophys.* **74**:326.
36. SMILLIE, R. M. 1960. *Nature.* **187**:1024.
37. RISKE, C. H., and Y. SUBBAROW. 1925. *J. Biol. Chem.* **66**:375.
38. SMILLIE, R. M., and R. C. FULLER. 1960. *Biochem. Biophys. Res. Commun.* **3**:368.
39. SAN PIETRO, A., and H. M. LANG. 1958. *J. Biol. Chem.* **231**:211.
40. SMILLIE, R. M. 1962. *Plant Physiol.* **37**:716.
41. JAMES, W. O., and V. S. R. DAS. 1957. *New Phytologist.* **54**:325.
42. ARNON, D. I. 1949. *Plant Physiol.* **24**:1.
43. CHANCE, B. 1957. In *Methods in Enzymology*. S. P. Colowick and N. O. Kaplan, editors. Academic Press Inc., New York. 4:273.
44. HILL, R., and W. D. BONNER. 1961. In *Light and Life*. W. D. McElory, and B. Glass, editors. The Johns Hopkins Press, Baltimore, 242.
45. BONNER, W. D., and R. HILL. 1963. *Photosynthesis Mechanisms in Green Plants*. *Natl. Acad. Sci. Natl. Res. Council. Publ.* **1145**.
46. WINTERMANS, J. F. G. M. 1960. *Biochim. Biophys. Acta.* **44**:49.
47. MARINETTI, G. V. 1965. *J. Lipid Res.* **6**:315.
48. BENSON, A. A., H. DANIEL, and R. WISER. 1959. *Proc. Natl. Acad. Sci. U. S.* **45**:1582.
49. OHAD, I., P. SIEKEVITZ, and G. E. PALADE. 1967. *J. Cell Biol.* **35**:553.
50. DUBOIS, M., K. A. GILLES, P. A. REBERS, and F. SMITH. 1956. *Anal. Chem.* **28**:350.
51. HORROKS, R. H. 1949. *Nature.* **164**:444.
52. LUFT, J. H. 1961. *J. Biophys. Biochem. Cytol.* **9**:409.
53. REYNOLDS, E. S. 1963. *J. Cell Biol.* **17**:208.
54. LOUD, A. V. 1962. *J. Cell Biol.* **15**:481.
55. OHAD, I., and D. DANON. 1964. *J. Cell Biol.* **22**:302.
56. HOHL, H. R., and A. HEPTON. 1965. *J. Ultrastruct. Res.* **12**:542.
57. WEIER, T. E., T. BISALPUTRA, and A. HARRISON. 1966. *J. Ultrastruct. Res.* **15**:38.
58. LYTTLETON, J. W. 1961. *Exptl. Cell Res.* **26**:312.
59. BRAWERMAN, G. 1963. *Biochim. Biophys. Acta.* **72**:317.
60. CLARK, M. F., R. E. F. MATTHEWS, and R. K. RALPH. 1964. *Biochim. Biophys. Acta.* **91**:289.
61. SPENCER, D. 1965. *Arch. Biochem. Biophys.* **111**:2.
62. HUDOCK, G. A., and R. P. LEVINE. 1964. *Plant Physiol.* **39**:889.
63. HUDOCK, G. A., G. C. MCLEOD, J. MORAKOVA-KIELY, and R. P. LEVINE. 1964. *Plant Physiol.* **39**:898.
64. SUEOKA, N. 1960. *Proc. Natl. Acad. Sci. U. S.* **46**:83.
65. BUFFALO, N. D. 1958. *Bull. Torrey Bot. Club.* **85**:157.
66. JACOBSON, B. S. 1962. *Radiation Res.* **17**:82.
67. JACOBSON, B. S., R. J. SALMON, and L. L. LANSKY. 1964. *Exptl. Cell Res.* **36**:1.

68. KATES, J. R., and R. F. JONES. 1964. *J. Cellular Comp. Physiol.* **63**:157.
69. SAGER, R., and G. E. PALADE. 1957. *J. Biophys. Biochem. Cytol.* **3**:463.
70. BEN-SHAUL, Y., T. H. EPSTEIN, and J. A. SCHIFF. 1965. *Can. J. Botany.* **43**:129.
71. VON WETTSTEIN, D. 1960. *Hereditas.* **46**:700.
72. GRANICK, S. 1950. *J. Biol. Chem.* **183**:713.
73. WOLFF, J. B., and L. PRICE. 1957. *Arch. Biochem. Biophys.* **72**:293.
74. SMILLIE, R. M. 1963. *Can. J. Botany.* **41**:123.
75. HALLAWAY, M. 1965. *Biol. Rev. Cambridge Phil. Soc.* **40**:188.
76. JAMES, W. O. R., and R. M. LEECH. 1964. *Proc. Roy. Soc. London Ser. B.* **160**:13.
77. SMILLIE, R. M., and R. P. LEVINE. 1963. *J. Biol. Chem.* **238**:4058.
78. LEVINE, R. P., and R. M. SMILLIE. 1963. *J. Biol. Chem.* **238**:4052.
79. PERINI, F., J. A. SCHIFF, and M. D. KAMEN. 1964. *Biochim. Biophys. Acta.* **88**:91.
80. PERINI, F., M. D. KAMEN, and J. A. SCHIFF. 1964. *Biochim. Biophys. Acta.* **88**:74.
81. FORTI, G., M. L. BERTOLE, and G. ZANETTI. 1965. *Biochim. Biophys. Acta.* **109**:33.
82. CARELL, E. F., and J. S. KAHN. 1964. *Arch. Biochem. Biophys.* **108**:1.
83. BRAWERMAN, G. E., and N. KONIGSBERG. 1960. *Biochim. Biophys. Acta.* **43**:374.
84. HAGEMAN, R. H., and D. I. ARNON. 1955. *Arch. Biochem. Biophys.* **57**:421.
85. MARGULIES, M. W. 1965. *Plant Physiol.* **40**:57.
86. HALL, D. O., R. C. HUFFAKER, L. M. SHANON, and A. WALLACE. 1959. *Biochim. Biophys. Acta.* **35**:540.
87. LEWIS, S. C., J. A. SCHIFF, and H. T. EPSTEIN. 1965. *J. Protozool.* **12**:281.
88. OHAD, I., P. SIEKEVITZ, and G. E. PALADE. 1966. *Federation Proc.* **25**(No. 2):225.